Design of a thermally stable succinonitrile mechanophore featuring electron-withdrawing triazine rings for radical polymerization

Hajime Sugita,[a] Akira Kodaka,[a] Akira Takahashi,[a] Koichiro Mikami*[b] and Hideyuki Otsuka*[a,c]

[a] Department of Chemical Science and Engineering, Institute of Science Tokyo, Meguro-ku, Tokyo 152-8550, Japan.

[b] Engineering Division, Process Device Innovation Center, Panasonic Industry Co., Ltd., 1006 Kadoma, Kadoma City, Osaka 571-8506, Japan.

[c] Research Center for Autonomous Systems Materialogy (ASMat), Institute of Integrated Research, Institute of Science Tokyo, 4259 Nagatsuta-cho, Midori-ku, Yokohama, Kanagawa 226-8501, Japan

*Corresponding author: E-mail: mikami.koichiro@jp.panasonic.com, otsuka@mct.isct.ac.jp

1. General Information

All reagents and solvents were purchased from Sigma-Aldrich, Wako Pure Chemical Industries, Tokyo Chemical Industry, or Kanto Chemical, and used as received, unless otherwise noted. ***t*-BuTACl** was synthesized according to a literature.[1] ^{1}H NMR spectra were obtained using a 500 MHz Bruker spectrometer. ^{13}C NMR spectra were obtained using a 500 MHz Bruker spectrometer. UV-vis absorption spectra were recorded with a JASCO V-650 equipped with an ISV-922 60 mm integrating sphere unite. Electron paramagnetic resonance (EPR) measurements were carried out on a JEOL JES-X320 X-band EPR spectrometer equipped with a JEOL DVT temperature controller. Gel permeation chromatography (GPC) measurements were carried out at 40 °C on TOSOH HLC-8420GPC EcoSEC Elite system equipped with a guard column (TOSOH TSK gel guard column Super H-L), three columns (TOSOH TSK gel SuperH 6000 and 2500×2) and a differential refractive index detector. Tetrahydrofuran (THF) was used as the eluent at a flow rate of 0.6 mL/min. Polystyrene (PS) standards (M_n = 4430–3242000; M_w/M_n = 1.03–1.08) were used to calibrate the GPC system. Grinding tests of *ca.* 60 mg of **BTASN-PMMA-H** for 10 min at 30 Hz were performed using a Retsch Mixer Mill MM 400 with a 10 mL of grinding jar and 5 mm stainless ball. Density functional theory (DFT) calculations were performed using Gaussian 16 program package[2] and Q-Chem 6.1.1 program package.[3]

2. Synthetic Procedures

2.1. Synthesis of ***t*-BuTACl**[1]

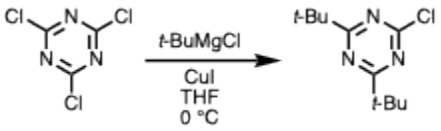

The two-necked flask equipped with dropwise funnel was heated under reduced pressure, and then cooled to room temperature under N_2 atmosphere. Cyanuric chloride (11.1 g, 60 .0 mmol) and copper (I) iodide (0.409 g, 2.15 mmol) were added, and the flask was vacuumed and backfilled with N_2. Dry THF (60 mL) was added with stream of N_2, and the solution was cooled at 0 °C. *tert*-BuMgCl solution in 1.0 M THF (150 mL, 150 mmol) was added by dropwise funnel at 0 °C for 40 min, and the reaction mixture was stirred at 0 °C for 3 h. The reaction was quenched by saturated NH_4Cl aqueous solution after dilution with Et_2O, and then the precipitation was filtrated with celite. The mixture was extracted with Et_2O, washed with water and brine, and dried over $MgSO_4$. After filtration, concentration under reduced pressure, and silica gel column chromatography purification (hexane/EtOAc; EtOAc = 0 to 5%) to afford ***t*-BuTACl** (10.3 g, 75%) as an off-white solid.

^{1}H NMR (500 MHz, $CDCl_3$): δ 1.37 (s, 18 H); ^{13}C NMR (125 MHz, $CDCl_3$) δ 187.7, 171.1, 39.8, 28.6.

2.2. Synthesis of **1**

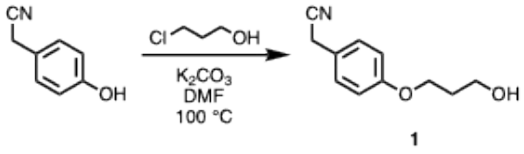

1

4-Hydroxybenzylcyanide (3.99 g, 30.0 mmol) and K_2CO_3 (8.23 g, 59.5 mmol) were added to the flask, and the flask was vacuumed and backfilled with N_2. Dry DMF (60 mL) was added with stream of N_2, and then the mixture was heated at 100 °C for 30 min. 3-Chloro-1-propanol (2.74 mL, 33.0 mmol) was added and the reaction mixture was stirred at 100 °C for 1 h. After cooling to room temperature, filtration and concentrated under reduced pressure, obtained crude products were purified by silica gel column chromatography purification (hexane/EtOAc; EtOAc = 40%) to afford **1** (4.88 g, 85%) as a white solid.

^{1}H NMR (500 MHz, $CDCl_3$): δ 7.22 (d, J = 8.7 Hz, 2 H), 6.90 (d, *J* = 8.7 Hz, 2 H), 4.11 (t, *J* = 6.0 Hz, 2 H), 3.85 (q, *J* = 5.6 Hz, 2 H), 3.67 (s, 2 H), 2.04 (quint, *J* = 6.0 Hz, 2 H), 1.80 (t, *J* = 5.0 Hz, 1 H); ^{13}C NMR (125 MHz, $CDCl_3$) δ 158.6, 129.1, 122.0, 118.2, 115.1, 65.7, 60.2, 32.0, 22.8. ESI-TOF MS (*m/z)*: $[M+Na]^+$ calcd. for $C_{11}H_{13}NNaO_2$, 214.0844; Found, 214.0838.

2.3. Synthesis of **2**

1 **2**

1 (3.83 g, 20.0 mmol) and imidazole (1.78 g, 26.2 mmol) were added to the flask, and the flask was vacuumed and backfilled with N_2. Dry DMF (20 mL) was added with stream of N_2, and then the mixture was cooled at 0 °C. *tert*-Butyldimethylchlorosilane (3.93g, 26.1 mmol) in dry CH_2Cl_2 (10.4 mL) solution was added dropwise at 0 °C, and the reaction mixture was stirred at room temperature for 4.5 h. The reaction was quenched by addition of saturated $NaHCO_3$ aqueous solution, and the mixture was extracted with mix solvent (hexane/EtOAc = 3/1). The organic layer was washed with water and brine, and dried over $MgSO_4$. After filtration and concentration under reduced pressure, obtained crude products were purified by silica gel column chromatography purification (hexane/EtOAc; EtOAc = 0 to 20%) to afford **2** (5.88 g, 96%) as a colorless oil.

^{1}H NMR (500 MHz, $CDCl_3$): δ 7.22 (d, *J* = 8.8 Hz, 2 H), 6.90 (d, *J* = 8.7 Hz, 2 H), 4.06 (t, *J* = 6.2 Hz, 2 H), 3.80 (t, *J* = 6.0 Hz, 2 H), 3.68 (s, 2 H), 2.04 (quint, *J* = 6.1 Hz, 2 H), 0.89 (s, 9 H), 0.04 (s, 6H); ^{13}C NMR (125 MHz, $CDCl_3$) δ 158.9, 129.1, 121.6, 118.2, 115.1, 64.6, 59.4, 32.3, 25.9, 22.8, 18.3, –5.4. ESI-TOF MS (*m/z)*: $[M+Na]^+$ calcd. for $C_{17}H_{27}NNaO_2Si$, 328.1709; Found, 328.1703.

2.4. Synthesis of **3**

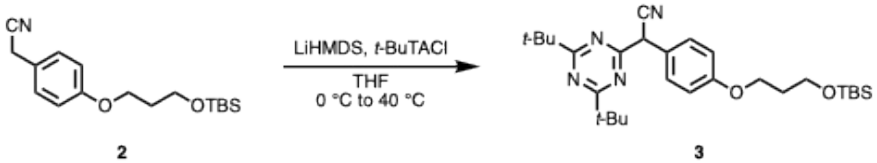

2 **3**

The schlenk flask was heated under reduced pressure, and then cooled to room temperature under N_2 atmosphere. **2** (0.9675 g, 3.17 mmol) was added to the flask, and the flask was vacuumed and

backfilled with N_2. After addition of dry THF (31.7 mL) with stream of N_2, the solution was cooled at 0 °C, and then 1.3 M of lithium bis(trimethylsilyl)amide (LiHMDS) in THF solution (4.90 mL, 6.37 mmol) was added dropwise. After stirred 30 min at 0 °C, ***t*-BuTACl** (0.7973 g, 3.50 mmol) was added with stream of N_2, the reaction mixture was stirred at 0 °C for 30 min, warm up to 40 °C, and stirred for 15 h. The reaction was quenched by neutralization by 2 M HCl at room temperature carefully (pH = 6–7), and the reaction mixture was extracted with EtOAc, washed brine, and dried over $MgSO_4$. After filtration and concentration under reduced pressure, obtained crude products were purified by silica gel column chromatography purification (hexane/CH_2Cl_2; CH_2Cl_2 = 50 to 100%) to afford **3 (**1.40 g, 94%) as an orange oil.

^{1}H NMR (500 MHz, $CDCl_3$): δ 7.49 (d. *J* = 8.7 Hz, 2 H), 6.89 (d, *J* = 8.9 Hz, 2 H), 5.17 (s, 1 H), 4.05 (t, *J* = 6.0 Hz, 2 H), 1.96 (quint, *J* = 6.10 Hz, 2 H), 1.35 (s, 18 H), 0.87 (s, 9 H), 0.03 (s, 6 H); ^{13}C NMR (125 MHz, $CDCl_3$) δ 186.1, 172.0, 159.4, 129.2, 125.0, 118.0, 115.0, 64.6, 59.4, 46.1, 39.7, 32.3, 28.8, 25.9, 18.3, –5.39. ESI-TOF MS (*m/z)*: $[M+Na]^+$ calcd. for $C_{28}H_{44}N_4NaO_2Si$, 519.3131; Found, 519.3126.

2.5. Synthesis of **4**

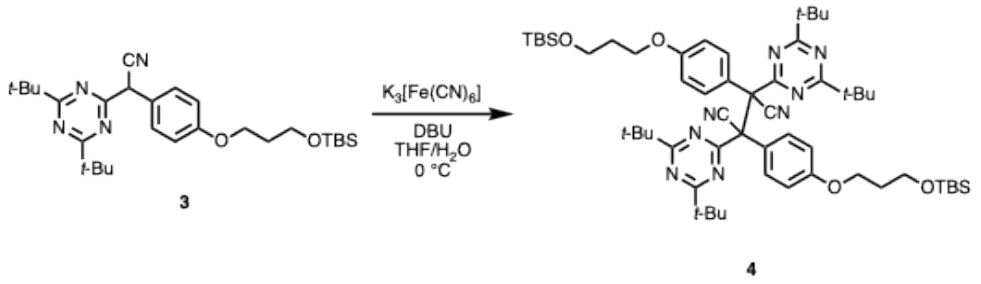

3 (1.06 g, 2.26 mmol) was added to the flask, and the flask was vacuumed and backfilled with N_2. After addition of dry THF (22.6 mL) mL was added with stream of N_2, the solution of 1,8-diazabicyclo[5.4.0]-7-undecene (DBU) (0.37 mL, 2.48 mmol) was added dropwise, and the mixture was stirred at room temperature. After stirred for 1 h, the solution was cooled to 0 °C. 0.50 M of $K_3[Fe(CN)_6]$ solution (4.97 mL, 2.49 mmol), which was prepared by of $K_3[Fe(CN)_6]$ (1.64 g, 4.99 mmol) with 10 mL measuring flask, was added dropwise to the solution, and the reaction mixture was stirred at 0 °C for 1 h. The reaction mixture was concentrated under reduced pressure, the obtained residue was dissolved EtOAc, and the organic layer was washed with water and brine, and dried over $MgSO_4$. After filtration and concentration under reduced pressure, obtained crude products (1.02 g, 91%) were purified by silica gel column chromatography purification (hexane/CH_2Cl_2; CH_2Cl_2 = 50 to 100%) to afford **4** (0.986 g, 88%) as a white solid.

^{1}H NMR (500 MHz, $CDCl_3$): δ 7.52 (d, J = 8.7 Hz, 1 H), 6.85–6.73 (m, 7 H), 4.06–3.99 (m, 4 H), 3.81–3.75 (m, 4 H), 2.01–1.92 (m, 4 H), 1.28–1.22 (m, 36 H), 0.88–0.87 (m, 18 H), 0.04–0.02 (m, 12 H); ^{13}C NMR (125 MHz, $CDCl_3$) δ 185.6, 174.0, 159.8, 131.0, 125.1, 118.4, 113.8, 64.5, 62.5, 59.5, 39.8, 32.3, 28.7, 25.9, 18.3, –5.37. ESI-TOF MS (*m/z)*: $[M+Na]^+$ calcd. for $C_{56}H_{86}N_8NaO_4Si_2$, 1013.6208; Found, 1013.6203.

2.6. Synthesis of **BTASN-OH**

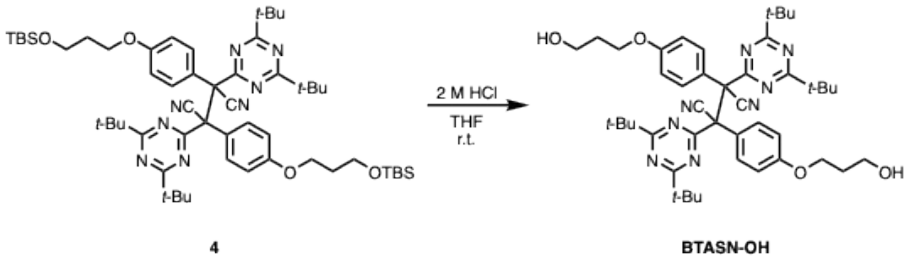

4 (762 mg, 0.77 mmol), dry THF (10.0 mL) and 2 M HCl (1.0 mL) were added to the flask, and the reaction mixture was stirred at room temperature for 3 h. The reaction was diluted by EtOAc,

and the organic layer was washed with water and brine, and dried over Na_2SO_4. After filtration and concentration under reduced pressure, obtained crude products were purified by silica gel column chromatography purification (hexane/EtOAc; EtOAc = 10 to 100%) and precipitation (CH_2Cl_2/hexane) to afford **BTASN-OH** 0.533 g (90%) as a white powder.

^{1}H NMR (500 MHz, $CDCl_3$): δ 6.86 (d, *J* = 9.0 Hz, 4 H), 6.79 (d, *J* = 9.1 Hz, 4 H), 4.12 (t, *J* = 6.0 Hz, 4 H), 3.86 (d, *J* = 5.2 Hz, 4 H), 2.05 (quin, *J* = 5.4 Hz, 4 H), 1.71 (s, 2 H), 1.22 (s, 36 H); ^{13}C NMR (125 MHz, $CDCl_3$) δ 185.7, 173.9, 159.3, 131.1, 125.4, 118.4, 113.8, 65.5, 62.5, 60.2, 39.8, 32.0, 28.7. ESI-TOF MS (*m/z*): $[M+Na]^+$ calcd. for $C_{44}H_{58}N_8NaO_4$, 785.4479; Found, 785.4473.

2.7. Synthesis of **BTASN-Int**

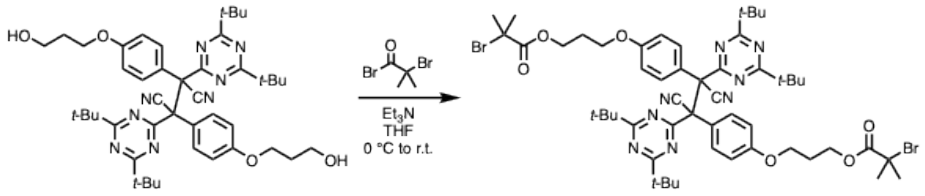

The two-necked flask was heated under reduced pressure, and then cooled to room temperature under N_2 atmosphere. **5** (154 mg, 0.20 mmol), dry THF (4.0 mL) and Et_3N (83 μL, 0.60 mmol) were added to the flask, and the solution was cooled at 0 °C, and then 2-bromoisobutyrylbromide (75 μL, 0.61 mmol) was added dropwise with stream of N_2 at 0 °C. After stirred for 3 h at 0 °C, the reaction mixture was diluted with EtOAc, and the precipitation was removed by filtration. The organic layer was concentrated under reduced pressure, and obtained residue was dissolved with EtOAc, and the organic layer was washed with 1 M HCl, saturated $NaHCO_3$ aq and brine, and dried over $MgSO_4$. After filtration and concentration under reduced pressure, obtained crude products were purified by silica gel column chromatography purification (hexane/EtOAc; EtOAc = 5 to 20%) and precipitation (EtOAc/(H_2O : MeOH = 1 : 1)) to afford **BTASN-Int** (105 mg, 50%) as a white powder.

^{1}H NMR (500 MHz, $CDCl_3$): δ 6.85 (d, *J* = 9.0 Hz, 4 H), 6.78 (d, *J* = 9.0 Hz, 4 H), 4.38 (t, *J* = 6.2 Hz, 4 H), 4.08 (t, *J* = 6.1 Hz, 4 H), 2.18 (quint, *J* = 6.1 Hz, 4 H), 1.934 (s, 6 H), 1.929 (s, 6 H), 1.22 (s, 36 H); ^{13}C NMR (125 MHz, $CDCl_3$) δ 185.7, 173.9, 171.6, 159.3, 131.1, 125.5, 118.4, 113.8, 64.2, 62.8, 62.4, 55.8, 39.8, 30.8, 28.7, 28.4. ESI-TOF MS (*m/z*): $[M+Na]^+$ calcd. for $C_{52}H_{68}Br_2N_8NaO_6$, 1081.3526; found, 1081.3521.

2.8. Synthesis of **BTASN-PMMA-Br**

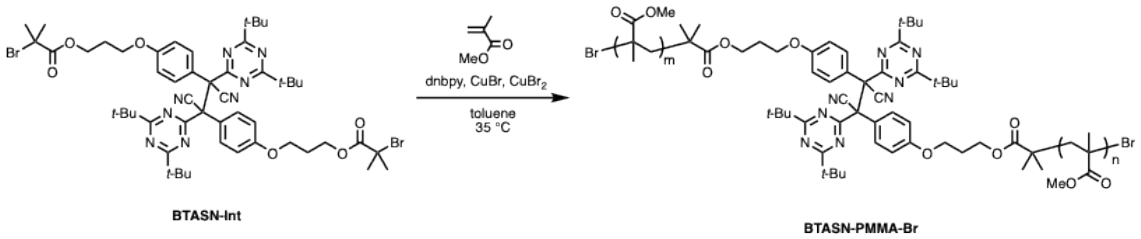

BTASN-Int **BTASN-PMMA-Br**

$CuBr_2$ (4.5 mg, 20.1 μmol), **BTASN-Int** (52.9 mg, 49.9 μmol), 4,4'-dinonyl-2,2'-bipyridyl (dnbpy) (98.8 mg, 241 μmol) were added to the Schlenk flask, and the flask was vacuumed and backfilled with N_2. Dry toluene (5.0 mL) and methyl methacrylate (MMA) (5.0 mL) were added with stream of N_2. The mixture was degassed by three times of freeze-pump-thaw cycling with liquid N_2 and left frozen after the third cycle. CuBr (14.3 mg, 99.7 μmol) was added under stream of N_2, and the flask was vacuumed and backfilled with N_2. After melting, the reaction mixture was stirred at 35 °C for 3.5 h. The reaction mixture was cooled at 0 °C for 10 min and exposed to air for 10 min at 0 °C. The solution was diluted by $CHCl_3$, filtrated through a column filled with neutral alumina, and concentrated under reduced pressure. The obtained residue was precipitated to hexane from $CHCl_3$ to afford **BTASN-PMMA-Br** as a white powder (677 mg, 14%, M_n = 14,200, M_w/M_n = 1.14).

2.9. Synthesis of **BTASN-PMMA-H**

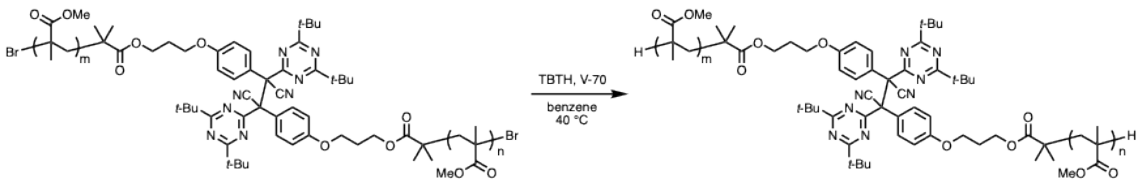

BTASN-PMMA-Br **BTASN-PMMA-H**

The atmosphere of Schlenk flask was replaced with N_2, and **BTASN-PMMA-Br** (491 mg, 33.0 μmol), benzene (33.0 mL) and tributyltin hydride (TBTH) (70.0 mg, 240 μmol) were added to the flask with stream of N_2. The mixture was degassed by three times of freeze-pump-thaw cycling and left frozen after the third cycle. V-70 (9.8 mg, 32 μmol) was added under stream of N_2, and the flask was vacuumed and backfilled with N_2 three times. After melting, the reaction mixture was stirred at 40 °C for 3 h. The reaction mixture was cooled at room temperature, diluted with CH_2Cl_2, and concentrated under reduced pressure. The obtained residue was precipitated to hexane from $CHCl_3$ and MeOH from $CHCl_3$ to afford **BTASN-PMMA-H** as a white powder (356

mg, 72%, M_n = 16,000, M_w/M_n = 1.08). The H ends were assigned according to the literatures.[4]

2.10. Synthesis of **BTASN-OH/PMMA-H**

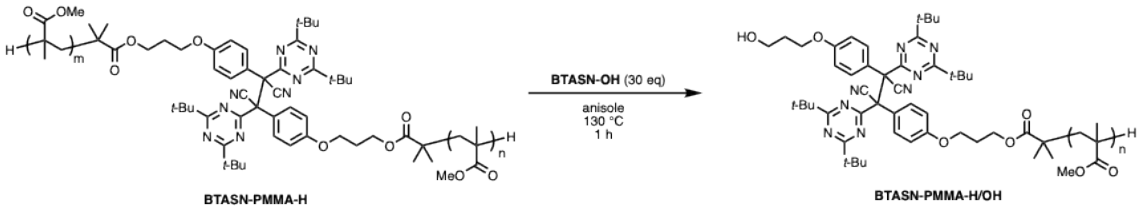

BTASN-PMMA-H (15.9 mg, 1.0 μmol), **BTASN-OH** (23.0 mg, 30 μmol) and anisole (2.0 mL) were added to the Schlenk flask, and the solution was degassed by three times of freeze-pump-thaw cycling, followed by stirring at 130 °C. After 1 h, the mixture was cooled at room temperature and concentrated under reduced pressure. GPC measurement of obtained residue was carried out without further purification (40.9 mg, M_n = 9,790, M_w/M_n = 1.10).

2.11. Synthesis of TASN series

The syntheses of TASNs were done via the potassium ferricyanide mediated coupling of substituted diarylacetonitriles (DAANs) with presence of base.

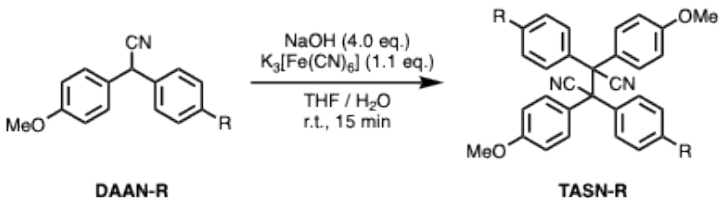

Synthesis of **DAAN-Me**

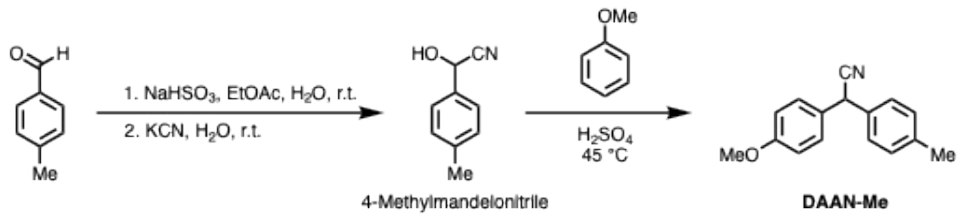

4-Methylmandelonitrile

In a two-neck round bottom flask, a solution of 4-tolualdehyde (7.07 mL, 60.0 mmol) in ethyl

acetate (120 mL) was formed. With stirring, a solution of sodium bisulfite (12.5 g, 120 mmol) in water (60.0 mL) was added at room temperature. The mixture was allowed to stir at room temperature for 1 h, and then a solution of KCN (7.81 g, 120 mmol) in water (120 mL) was added dropwise at 0 °C. Once the additional was complete, the mixture was allowed to stir for another 16 h as it warmed to room temperature. The reaction mixture was extracted with ethyl acetate, then the combined organic extracts were washed with brine and were dried over Na_2SO_4. After concentration, the residue was recrystallized from a mixed solvent of chloroform and hexane. The precipitate collected by filtration was dried in vacuo to give 4-methylmandelonitrile as a white crystal (7.56 g, 86% yield).

^{1}H NMR (500 MHz, CDCl3): δ 7.46–7.41 (m, 2H), 7.26–7.25 (m, 2H), 5.51 (d, *J* = 7.2 Hz, 1H), 2.56 (d, *J* = 7.2 Hz, 1H), 2.39 (s, 3H). ^{13}C NMR (100 MHz, $CDCl_3$): δ 139.94, 132.26, 129.84, 126.74, 119.13, 63.30, 21.28.

DAAN-Me

In a two-neck round bottom flask, 4-methylmandelonitrile (501 mg, 3.0 mmol) was dissolved in anisole (2.5 mL, 23 mmol). With stirring, 96% sulfuric acid (80 μL) was added, and the mixture was allowed to stir at 45 °C for 48 h. After cooling to room temperature, the liquid was decanted and the remaining solid was dissolved in ethyl acetate. The solution was washed with water and brine, and then dried over Na_2SO_4. After concentration, the residue was recrystallized from mixed solvent of chloroform and hexane, the precipitate collected by filtration was dried in vacuo. After that, the residue was recrystallized from a mixed solvent of chloroform and hexane. The precipitate collected by filtration was dried in vacuo to give **DAAN-Me** as a white powder (360 mg, 72% yield).

^{1}H NMR (500 MHz, $CDCl_3$): δ 7.25–7.22 (m, 4H), 7.16 (d, *J* = 7.8 Hz, 2H), 6.88 (d, *J* = 8.4 Hz, 2H), 5.05 (s, 1H), 3.79 (s, 3H), 2.33 (s, 3H). ^{13}C NMR (100 MHz, $CDCl_3$): δ 159.50, 138.08, 133.45, 129.93, 128.95, 128.35, 127.62, 120.24, 114.62, 55.45, 41.57, 21.19. FT-IR (KBr, cm^{-1}): 2961, 2932, 2841, 2243, 1889, 1657, 1610, 1581, 1511, 1452, 1300, 1265, 1179, 1112, 1028, 975, 870, 843, 813, 761, 698, 634, 598, 532, 505, 422. EI-MS (*m/z*): $[M]^+$ calcd. for $C_{16}H_{15}NO$, 237.1155; found, 237.1154.

Synthesis of **DAAN-CN**

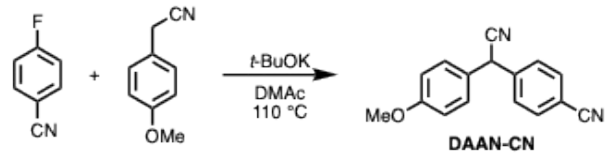

DAAN-CN

Under a nitrogen atmosphere, *t*-BuOK (18.1 g, 161 mmol) was dissolved in dry DMAc (140 mL) at 110 °C. After 15 min, 4-methoxyphenylacetonitrile (5.44 mL, 40.3 mmol) and 4-fluorobenzonitrile (7.32 mg, 60.4 mmol) were added. The reaction mixture was stirred for 4 h at 110 ºC. The reaction mixture was cooled to room temperature and then poured into water. The mixture was neutralized to pH 7 using HCl aq., extracted with toluene, washed with water and brine, dried over anhydrous Na_2SO_4. After concentration, the residue was recrystallized from a mixed solvent of chloroform and hexane. The precipitate collected by filtration was dried in vacuo. After that, the residue was recrystallized from a mixed solvent of chloroform and hexane. The precipitate collected by filtration was dried in vacuo to give **DAAN-CN** as a white crystal (6.40 g, 64% yield).

^{1}H NMR (500 MHz, $CDCl_3$): δ/ppm 7.67 (d, *J* = 8.1 Hz, 2H), 7.47 (d, *J* = 8.0 Hz, 2H), 7.22 (d, *J* = 8.4, 2H), 6.91 (d, *J* = 8.4 Hz, 2H), 5.14 (s, 1H), 3.81 (s, 3H). ^{13}C NMR (100 MHz, $CDCl_3$): δ 159.92, 141.47, 133.03, 129.06, 128.52, 126.60, 118.98, 118.26, 114.97, 112.37, 55.51, 41.84. FT-IR (KBr, cm^{-1}): 3741, 2962, 2914, 2363, 2236, 1609, 1509, 1452, 1415, 1297, 1262, 1179, 1116, 1025, 870, 830, 806, 768, 695, 596, 568, 544, 517. EI-MS (*m/z*): $[M]^+$ calcd. for $C_{16}H_{12}N_2O$, 248.0950; found, 248.0945.

Synthesis of **DAAN-Ac**

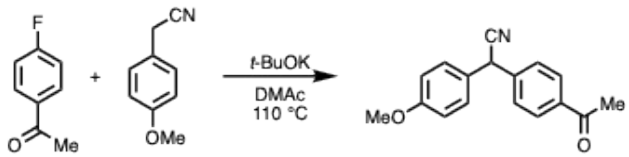

DAAN-Ac

Under a nitrogen atmosphere, *t*-BuOK (16.9 g, 151 mmol) was dissolved in dry DMAc (150 mL) at 110 °C. After 15 min, 4-methoxyphenylacetonitrile (5.09 mL, 37.7 mmol) and 4-fluoroacetophenone (6.62 mL, 56.5 mmol) were added. The reaction mixture was stirred for 4 h at 110 ºC. The reaction mixture was cooled to room temperature and then poured into water. The mixture was neutralized to pH 7 using HCl aq., extracted with toluene, washed with water and brine, dried over anhydrous Na_2SO_4. After concentration, the residue was recrystallized from a

mixed solvent of chloroform and hexane. The precipitate collected by filtration was dried in vacuo. After that, the residue was recrystallized from a mixed solvent of chloroform and hexane. The precipitate collected by filtration was dried in vacuo to give **DAAN-Ac** as a white crystal (7.83 g, 78% yield).

^{1}H NMR (500 MHz, $CDCl_3$): δ 7.96 (d, J = 8.1 Hz, 2H), 7.45 (d, J = 8.1 Hz, 2H), 7.24 (d, J = 8.8 Hz, 2H), 6.90 (d, J = 8.8 Hz, 2H), 5.14 (s, 1H), 3.80 (s, 3H), 2.59 (s, 3H). ^{13}C NMR (100 MHz, $CDCl_3$): δ 197.32, 159.74, 141.27, 136.88, 129.24, 129.00, 127.96, 127.22, 119.40, 114.82, 55.46, 41.79, 26.77. FT-IR (KBr, cm^{-1}): 3741, 2962, 2364, 2247, 1685, 1607, 1512, 1456, 1419, 1360, 1302, 1265, 1180, 1116, 1026, 958, 827, 804, 768, 731, 693, 601, 519. EI-MS (m/z): $[M]^+$ calcd. for $C_{17}H_{15}NO_2$, 265.1103; found, 265.1103.

Synthesis of **DAAN-OMe**

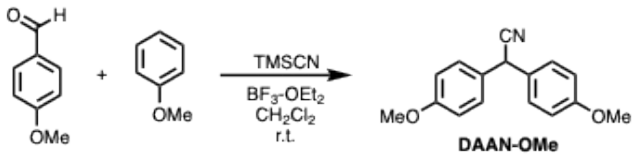

To a well-mixed solution of 4-methoxybenzaldehyde (4.80 mL, 39.5 mmol), anisole (5.12 mL, 47.4 mmol), and trimethylsilyl cyanide (7.34 mL, 59.2 mmol) in CH_2Cl_2 (200 mL) at 0 °C was added BF_3-OEt_2 (5.95 mL, 47.4 mmol). After being stirred at room temperature for 5.5 h, the reaction mixture was diluted with CH_2Cl_2, washed with aq. $NaHCO_3$ and water. The organic layers were collected, dried over $MgSO_4$. After concentration, the residue was recrystallized from a mixed solvent of chloroform and hexane, the precipitate collected by filtration was dried in vacuo to give **DAAN-OMe** as a white crystal (8.22 g, 82% yield).

^{1}H NMR (500 MHz, $CDCl_3$): δ 7.23 (d, J = 8.6 Hz, 4H), 6.89 (d, J = 8.5 Hz, 4H), 5.04 (s, 1H), 3.79 (s, 6H). ^{13}C NMR (100 MHz, $CDCl_3$): δ 159.45, 128.89, 128.37, 120.23, 114.57, 55.45, 41.15. FT-IR (NaBr, cm^{-1}) : 3052, 3005, 2964, 2934, 2899, 2838, 2243, 1889.9, 1609, 1582, 1446, 1334, 1177 , 1115, 970, 865, 812, 808, 768, 632, 595, 542, 512. EI-MS (m/z): $[M]^+$ calcd. for $C_{16}H_{15}NO_2$, 253.1103; found, 253.1102.

Syntheses of **TASN-Me, TASN-CN, TASN-Ac, TASN-OMe**

As a general method, DAAN and tetrahydrofuran was added to a two-neck flask under nitrogen atmosphere. With stirring, potassium ferricyanide (1.1 eq.) in 5 M NaOH aqueous solution (4.0 eq.) was added dropwise at room temperature. Then, the mixture was allowed to stir for 15 minutes at room temperature. After filtration, the residual was washed with water. After the crude solid was reprecipitated in methanol from THF for three times, the resulting precipitate was filtrated and dried in vacuo to give TASN as a white powder.

TASN-Me (78%)

^{1}H NMR (500 MHz, 1,1,2,2-tetrachloroethane-d_2): δ 7.03–7.20 (m, 6H), 6.74–6.80 (m, 2H), 3.80 (s, 3H), 2.34 (s, 3H). ^{13}C NMR (100 MHz, $CDCl_3$): δ 159.43, 159.37, 138.39, 138.32, 134.49, 134.42, 131.49, 131.39, 129.99, 129.89, 129.34, 129.27, 128.82, 128.74, 121.55, 113.31, 113.23, 58.65, 55.36, 21.09. ESI-TOF MS (*m/z*): $[M+Na]^+$ calcd. for $C_{32}H_{28}N_2NaO_2$: 495.2043; Found, 495.2038.

TASN-CN (99%)

^{1}H NMR (500 MHz, 1,1,2,2-tetrachloroethane-d_2): δ 7.58–7.63 (m, 2H), 7.37–7.43 (m, 2H), 7.08–7.14 (m, 2H), 6.80–6.86 (m, 2H), 3.82 (s, 3H). ^{13}C NMR (100 MHz, $CDCl_3$): δ 160.18, 141.92, 132.09, 131.95, 131.33, 131.14, 130.80, 130.59, 126.87, 126.78, 120.14, 117.87, 117.71, 114.11, 113.97, 113.24, 113.06, 58.70, 55.50, 31.67, 22.74, 14.22. ESI-TOF MS (*m/z*): $[M+Na]^+$ calcd. for $C_{32}H_{22}N_4NaO_2$: 517.1635; Found, 517.1642.

TASN-Ac (89%)

^{1}H NMR (500 MHz, 1,1,2,2-tetrachloroethane-d_2): δ 7.82–7.88 (m, 2H), 7.38–7.48 (m, 2H), 7.06–7.17 (m, 2H), 6.77–6.85 (m, 2H), 3.79–3.83 (m, 3H), 2.57–2.62 (m, 3H). ^{13}C NMR (100 MHz, $CDCl_3$): δ 197.28, 159.90, 141.96, 136.93, 131.49, 131.24, 130.40, 130.16, 128.21, 128.02, 127.76, 120.68, 113.81, 113.61, 58.84, 55.43, 26.78. ESI-TOF MS (*m/z*): $[M+Na]^+$ calcd. for $C_{24}H_{28}N_2NaO_4$: 551.1941; Found, 551.1927.

TASN-OMe (81%)

^{1}H NMR (500 MHz, 1,1,2,2-tetrachloroethane-d_2): δ 7.16 (d, J = 8.90 Hz, 4H), 6.78 (d, J = 8.92 Hz, 4H), 3.80 (s, 6H). ^{13}C NMR (100 MHz, 1,1,2,2-tetrachloroethane-d_2): δ 159.32, 131.45, 129.30, 121.57, 113.43, 58.48, 55.61. ESI-TOF MS (*m/z*): $[M+Na]^+$ calcd. for $C_{32}H_{28}N_2NaO_4$: 527.1941; Found, 527.1950.

3. NMR spectra

^{1}H NMR spectra

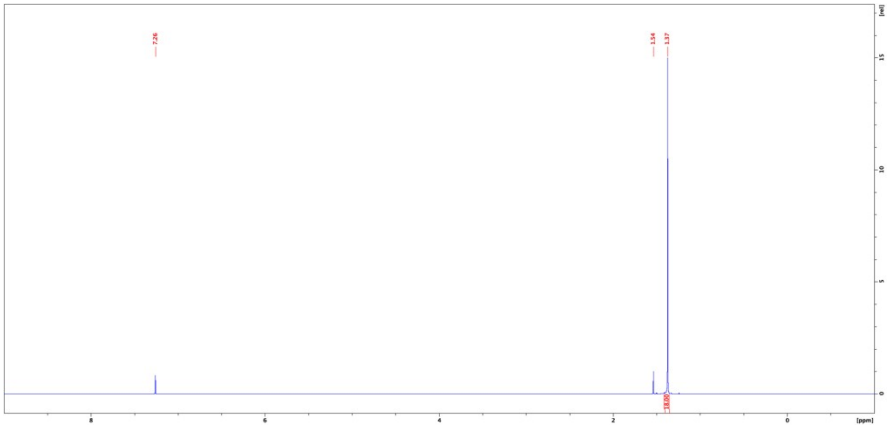

Figure S1. ^{1}H NMR spectrum of ***t*BuTACl** (500 MHz, $CDCl_3$).

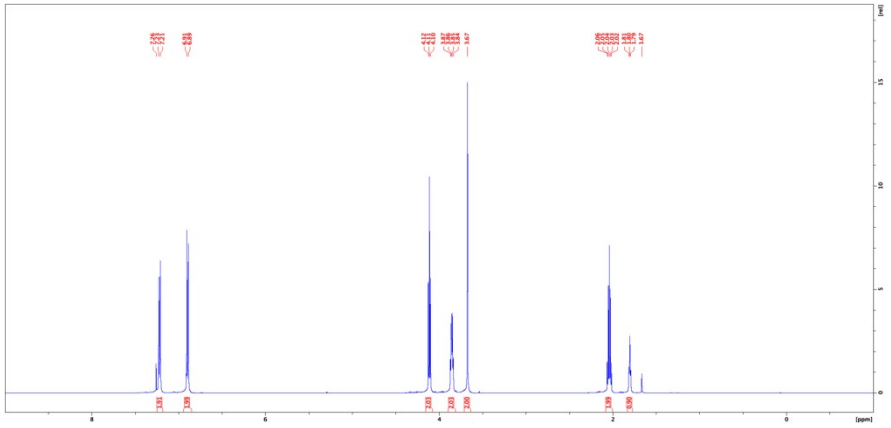

Figure S2. ^{1}H NMR spectrum of **1** (500 MHz, $CDCl_3$).

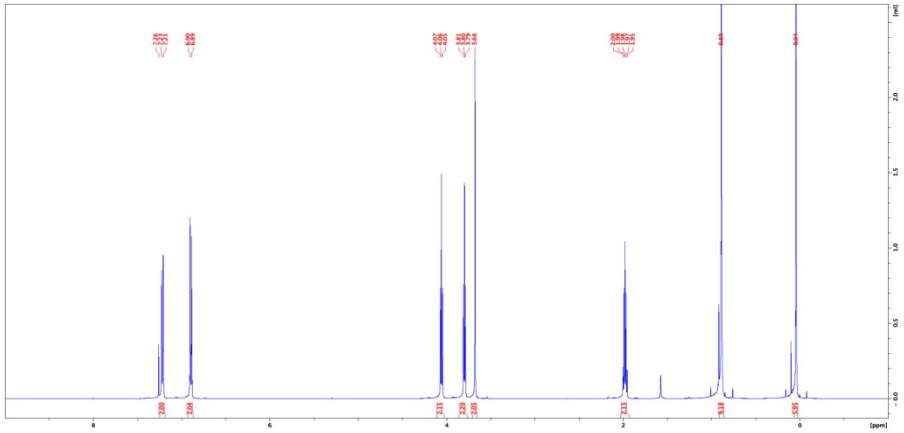

Figure S3. ^{1}H NMR spectrum of **2** (500 MHz, $CDCl_3$).

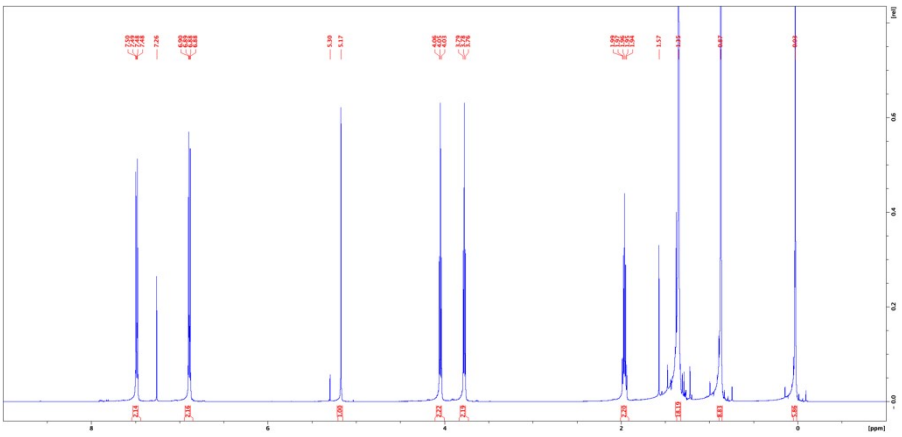

Figure S4. ^{1}H NMR spectrum of **3** (500 MHz, $CDCl_3$).

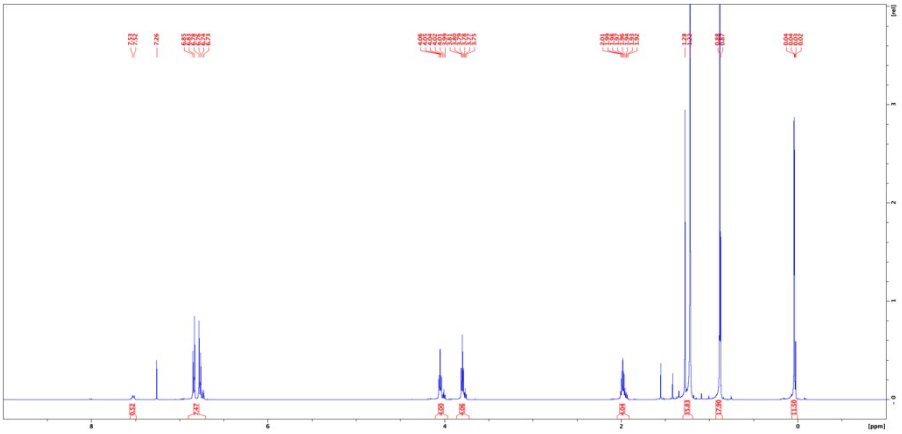

Figure S5. ^{1}H NMR spectrum of **4** (500 MHz, $CDCl_3$).

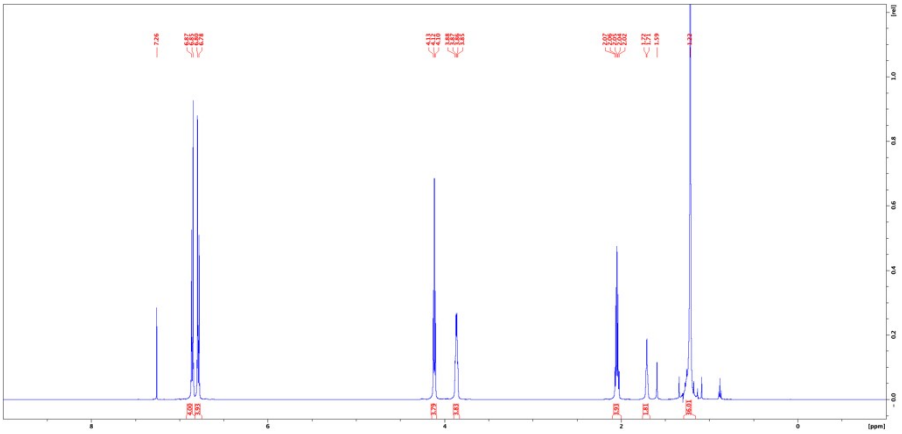

Figure S6. ^{1}H NMR spectrum of **BTASN-OH** (500 MHz, $CDCl_3$).

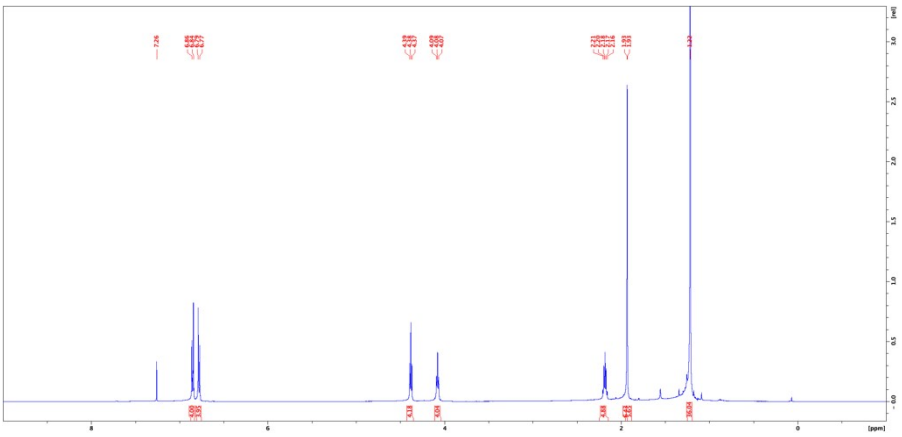

Figure S7. ^{1}H NMR spectrum of **BTASN-Int** (500 MHz, $CDCl_3$).

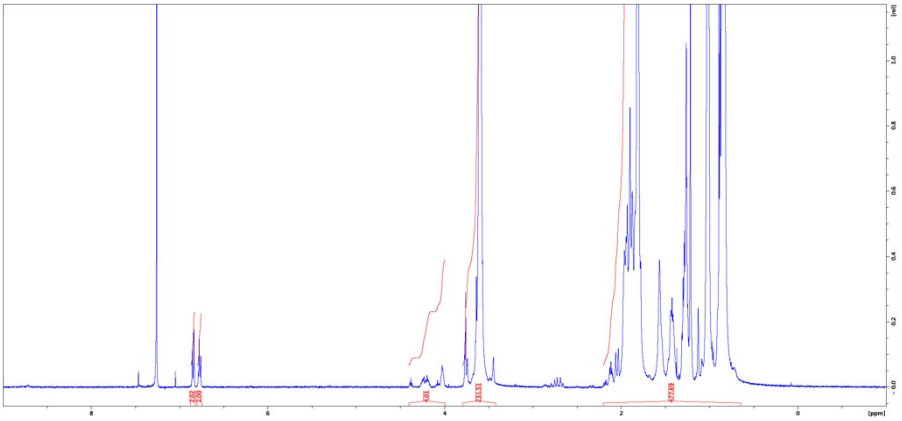

Figure S8. ^{1}H NMR spectrum of **BTASN-PMMA-Br** (500 MHz, $CDCl_3$).

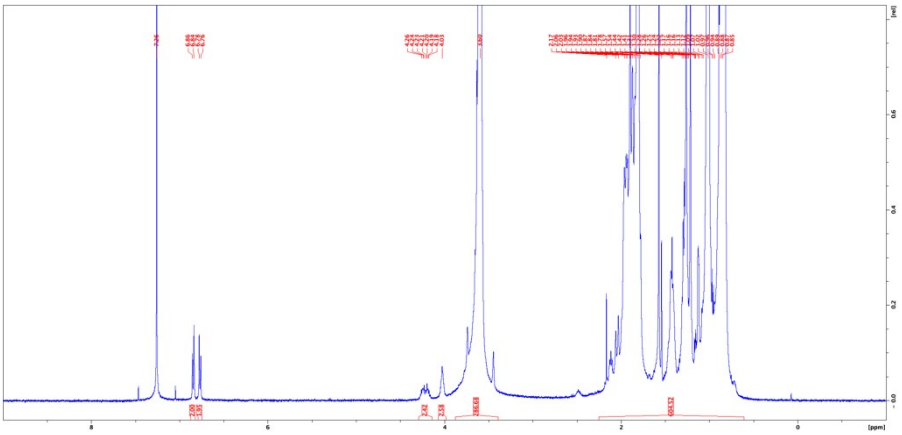

Figure S9. ^{1}H NMR spectrum of **BTASN-PMMA-H** (500 MHz, $CDCl_3$).

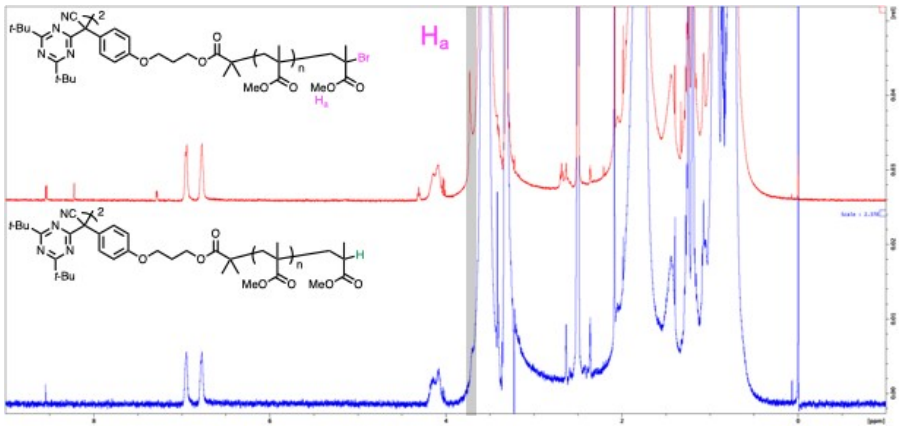

Figure S10. ^{1}H NMR spectra of **BTASN-PMMA-Br** (top) and **BTASN-PMMA-H** (bottom) (500 MHz, DMSO-d_6).

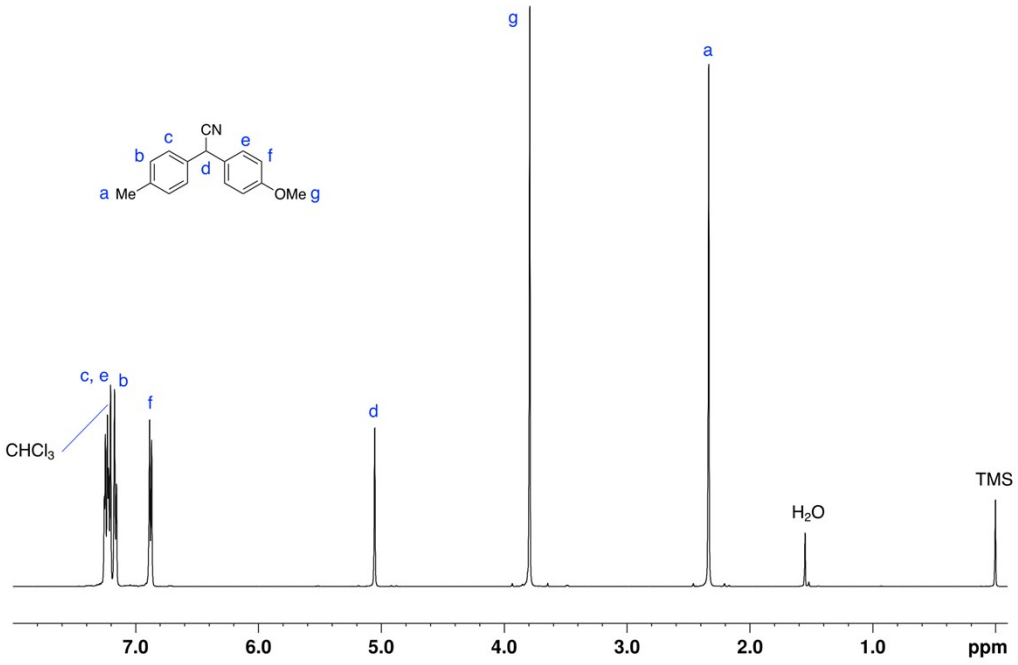

Figure S11. ^{1}H NMR spectrum of **DAAN-Me** (500 MHz, $CDCl_3$).

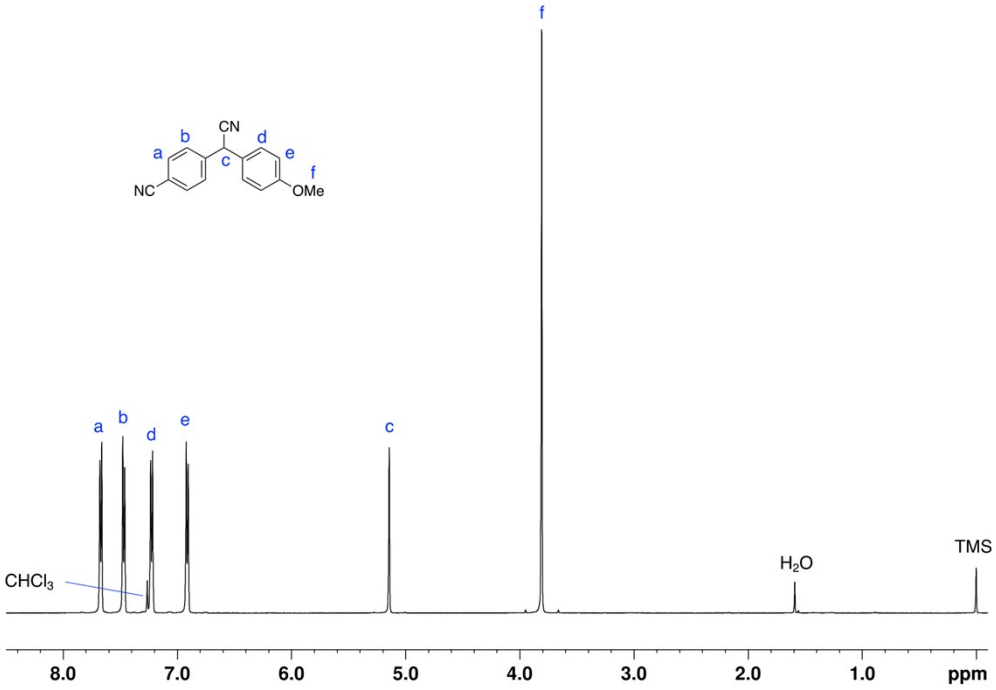

Figure S12. ^{1}H NMR spectrum of **DAAN-CN** (500 MHz, $CDCl_3$).

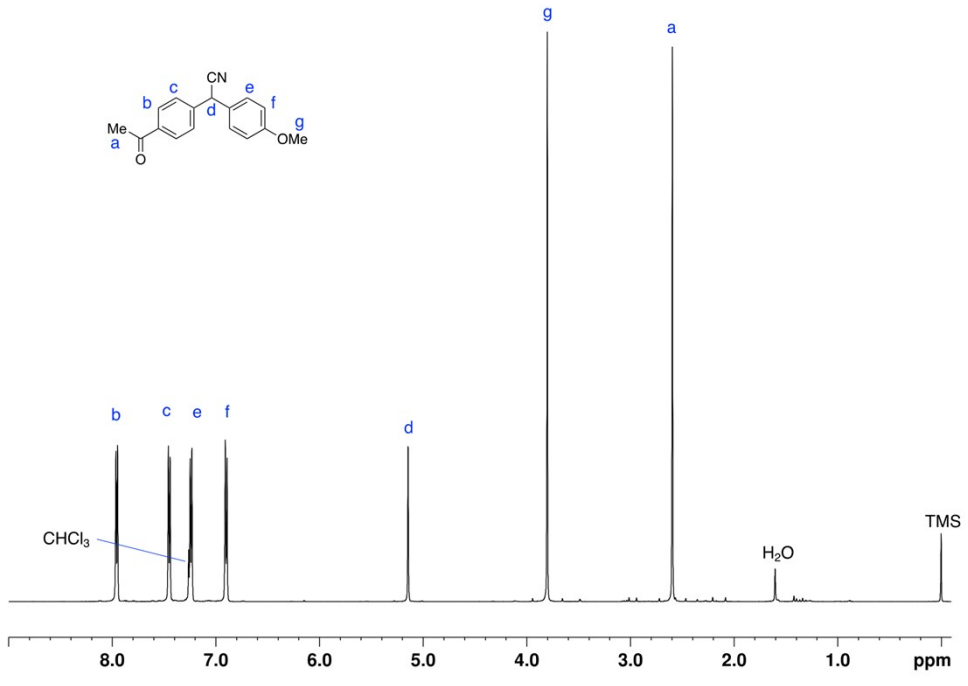

Figure S13. ^{1}H NMR spectrum of **DAAN-Ac** (500 MHz, $CDCl_3$).

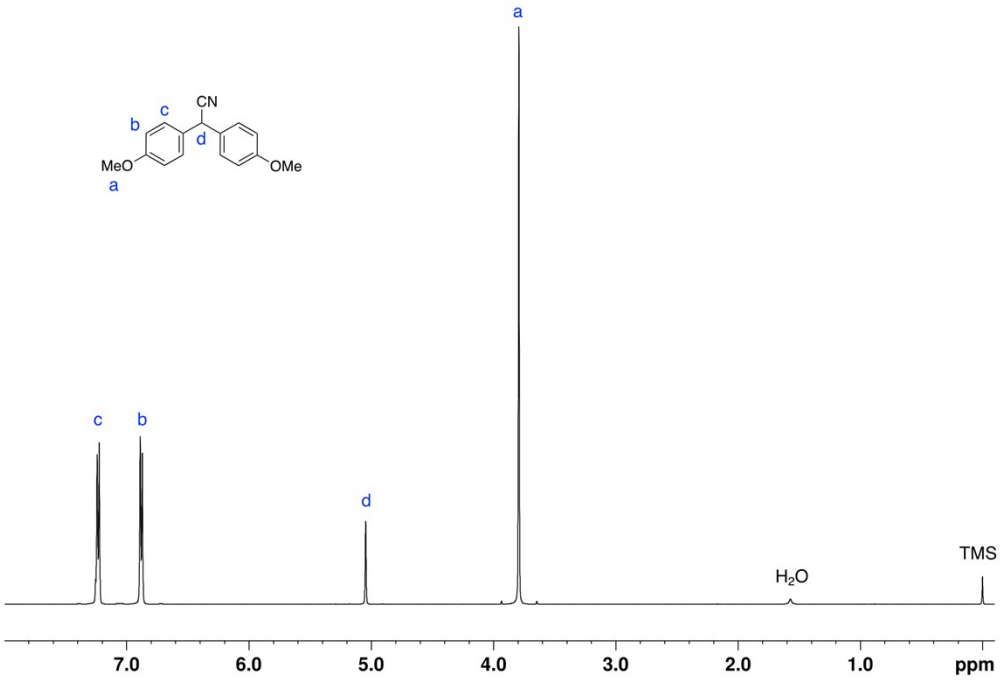

Figure S14. [1]H NMR spectrum of **DAAN-OMe** (500 MHz, $CDCl_3$).

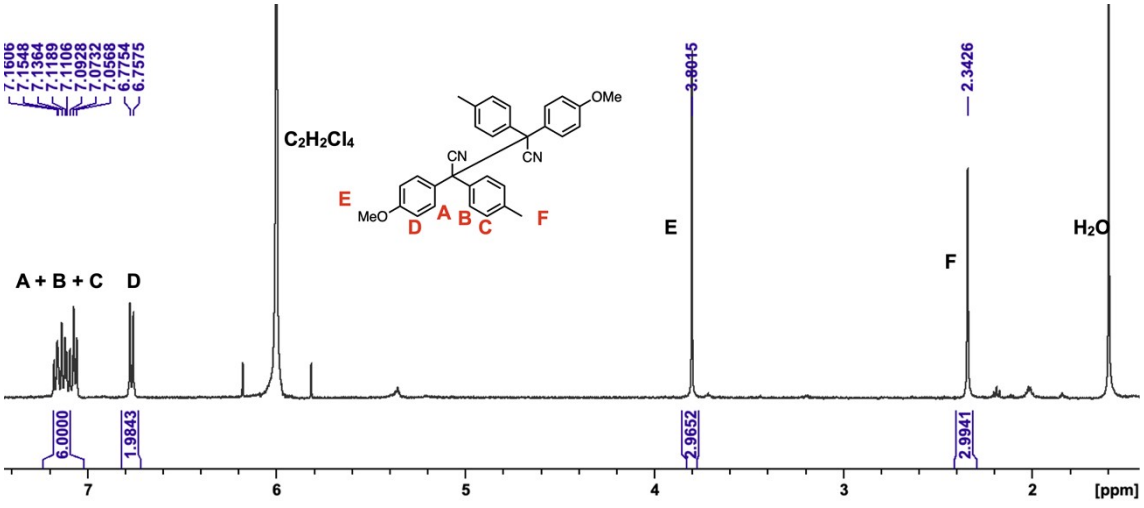

Figure S15. [1]H NMR spectrum of **TASN-Me** (500 MHz, 1,1,2,2-tetrachloroethane-d_2).

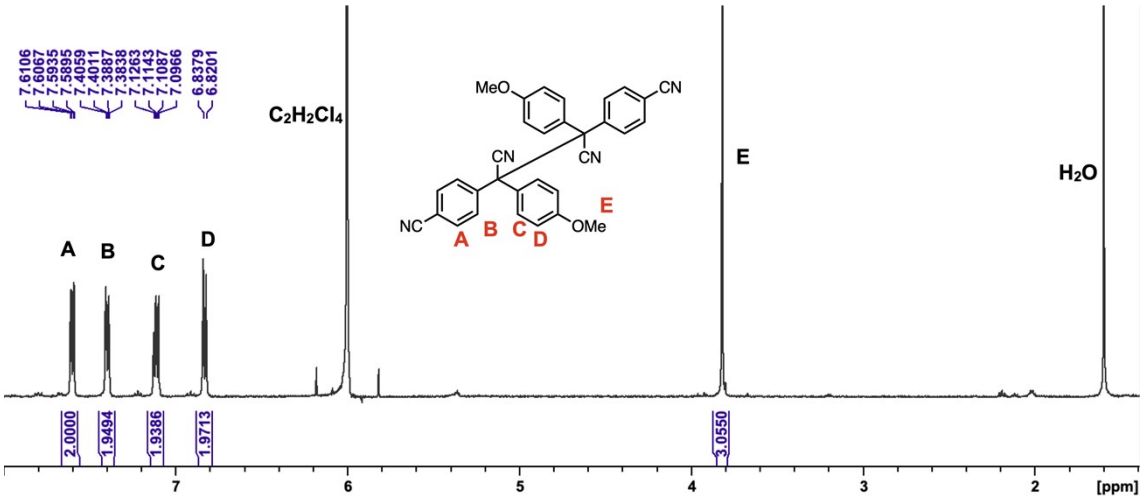

Figure S16. ^{1}H NMR spectrum of **TASN-CN** (500 MHz, 1,1,2,2-tetrachloroethane-d_2).

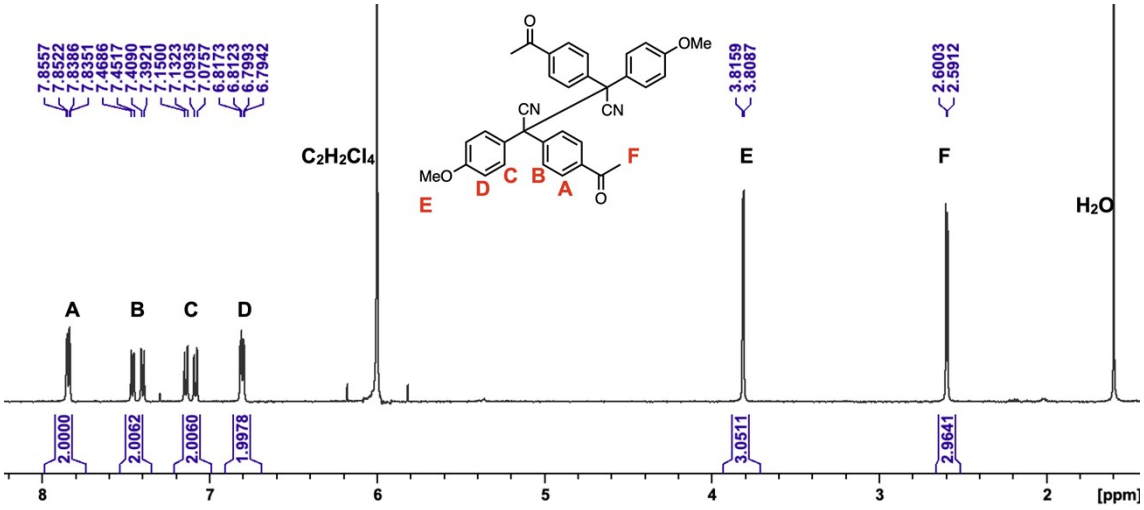

Figure S17. ^{1}H NMR spectrum of **TASN-Ac** (500 MHz, 1,1,2,2-tetrachloroethane-d_2).

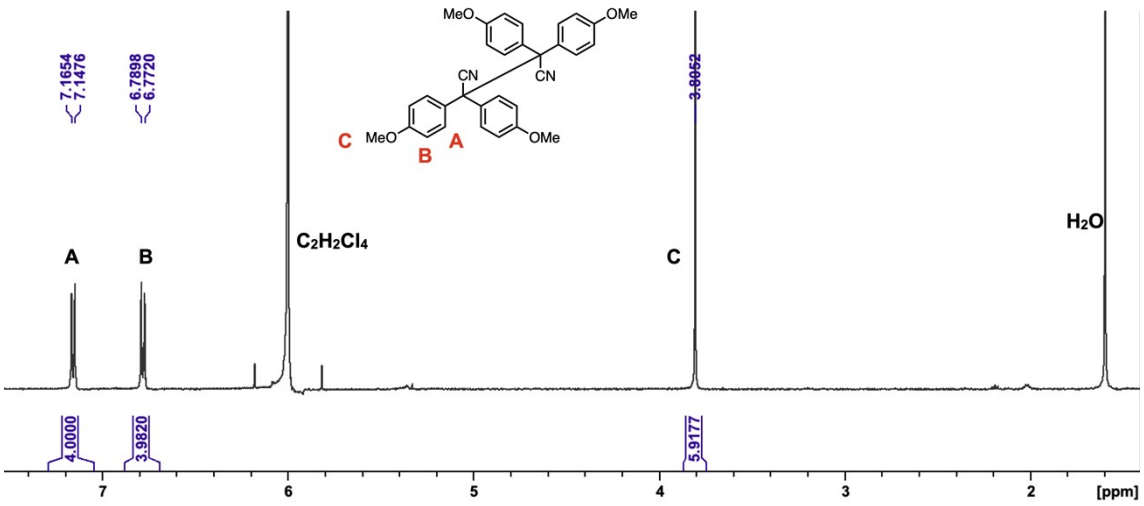

Figure S18. [1]H NMR spectrum of **TASN-OMe** (500 MHz, 1,1,2,2-tetrachloroethane-d_2).

[13]C NMR spectra

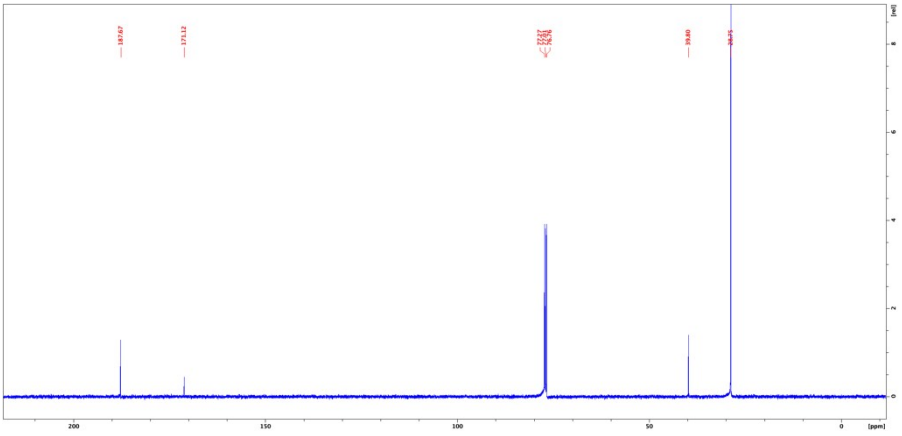

Figure S19. [13]C NMR spectrum of ***t*BuTACl** (125 MHz, $CDCl_3$).

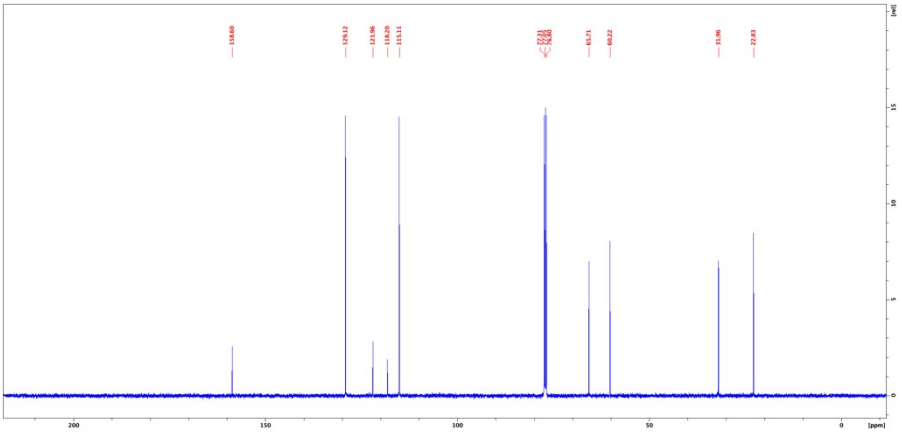

Figure S20. ^{13}C NMR spectrum of **1** (125 MHz, $CDCl_3$).

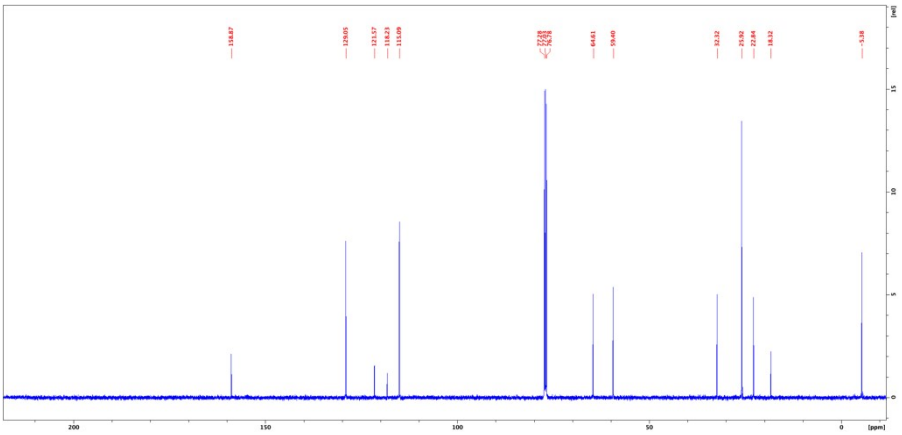

Figure S21. ^{13}C NMR spectrum of **2** (125 MHz, $CDCl_3$).

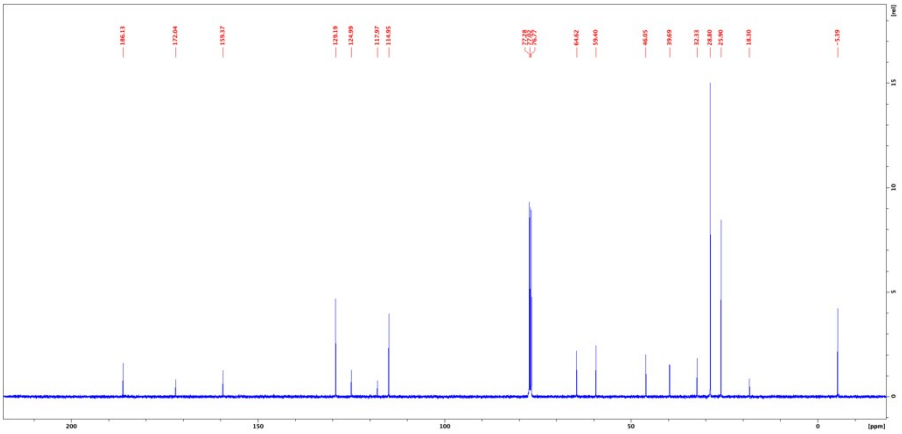

Figure S22. ^{13}C NMR spectrum of **3** (125 MHz, $CDCl_3$).

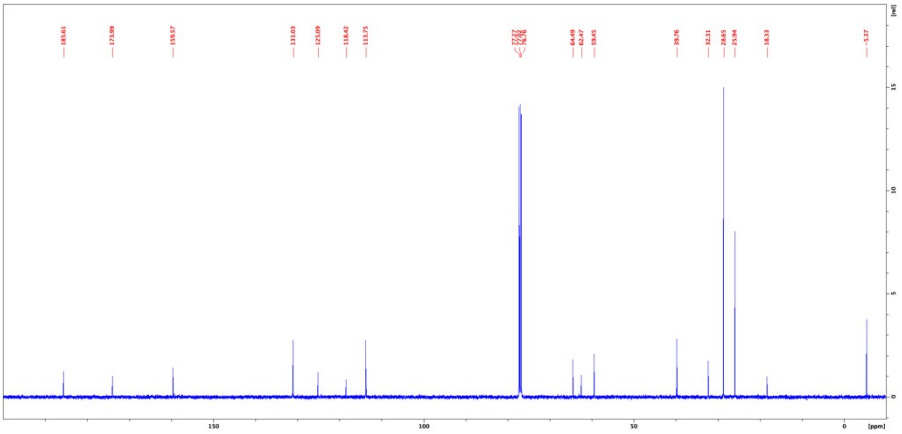

Figure S23. ^{13}C NMR spectrum of **4** (125 MHz, $CDCl_3$).

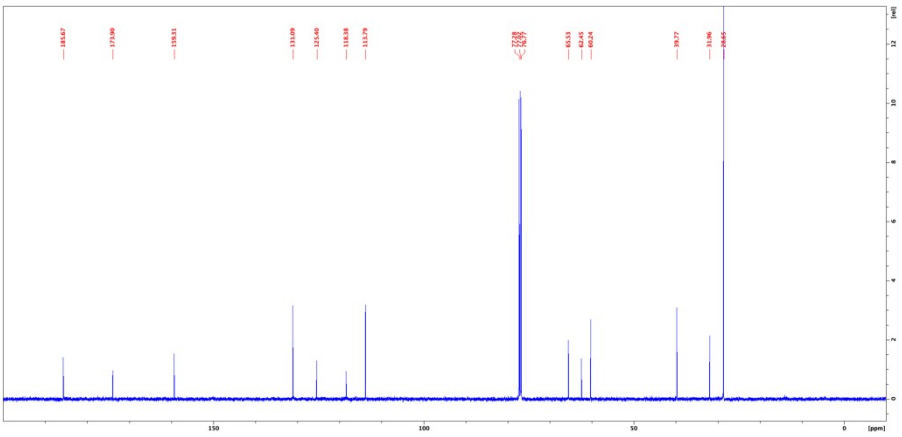

Figure S24. ^{13}C NMR spectrum of **BTASN-OH** (125 MHz, $CDCl_3$).

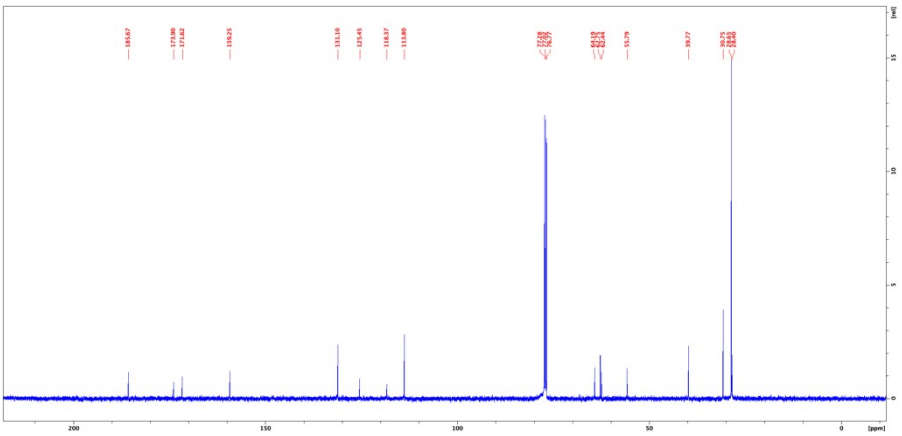

Figure S25. ^{13}C NMR spectrum of **BTASN-Int** (125 MHz, $CDCl_3$).

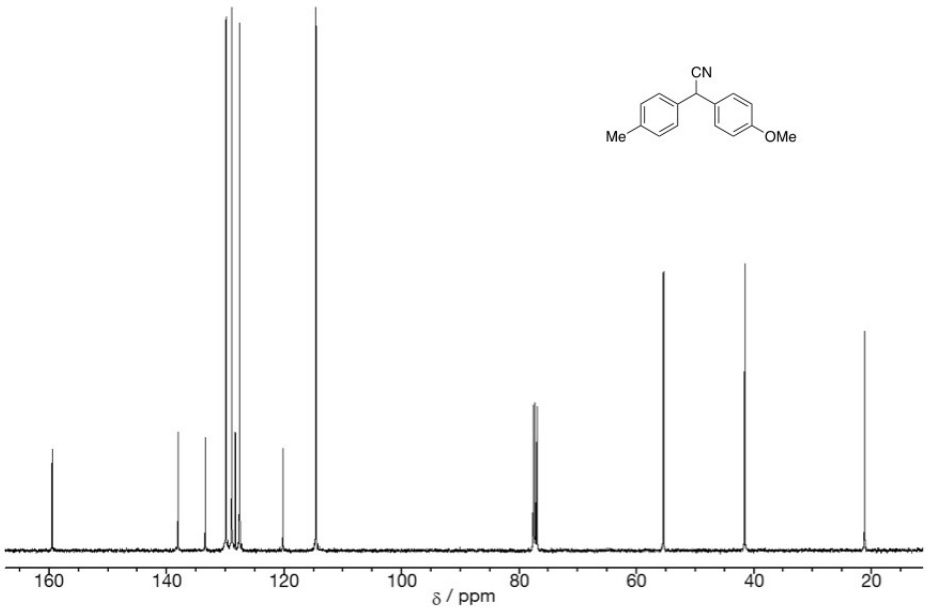

Figure S26. ^{13}C NMR spectrum of **DAAN-Me** (125 MHz, $CDCl_3$).

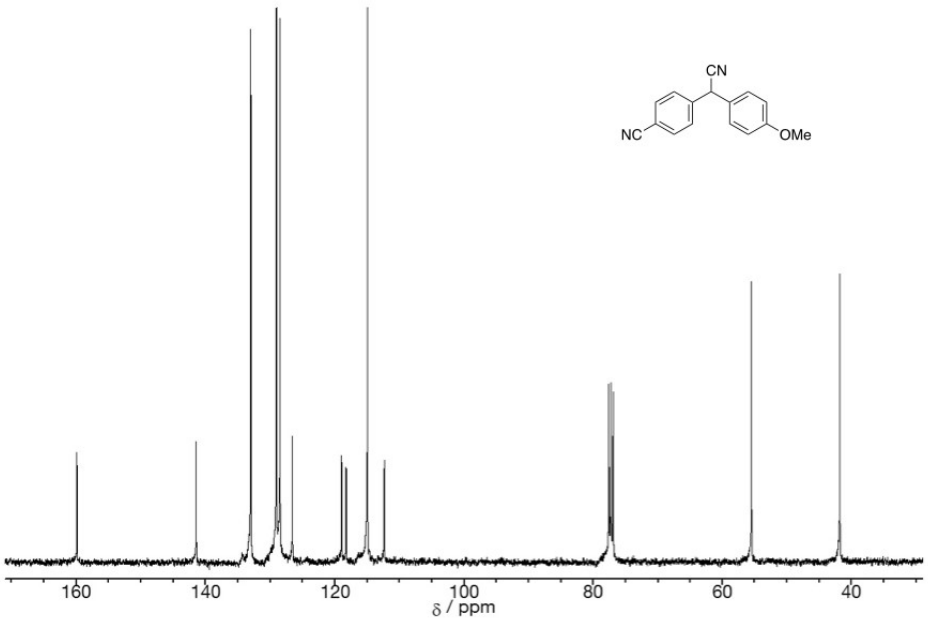

Figure S27. ^{13}C NMR spectrum of **DAAN-CN** (125 MHz, $CDCl_3$).

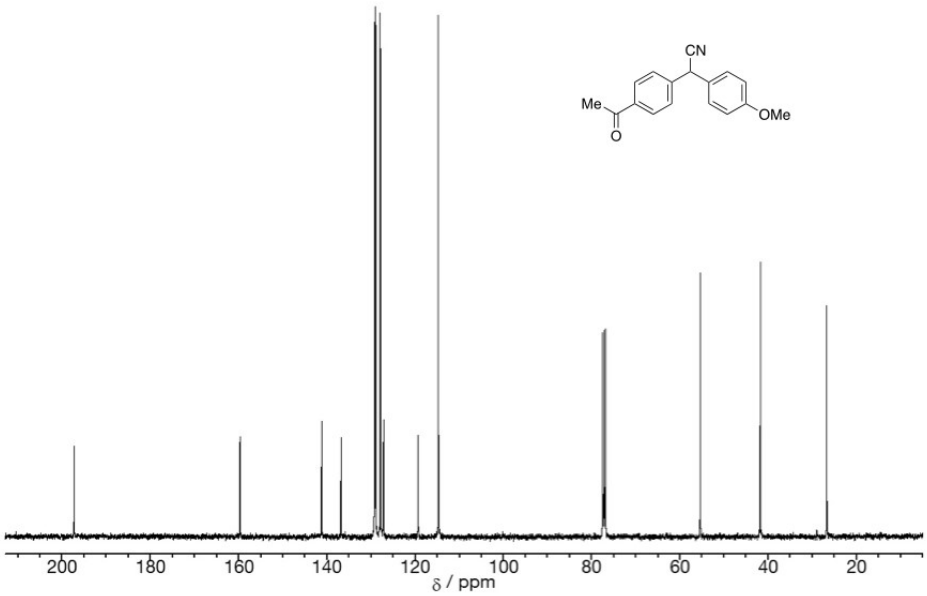

Figure S28. ^{13}C NMR spectrum of **DAAN-Ac** (125 MHz, $CDCl_3$).

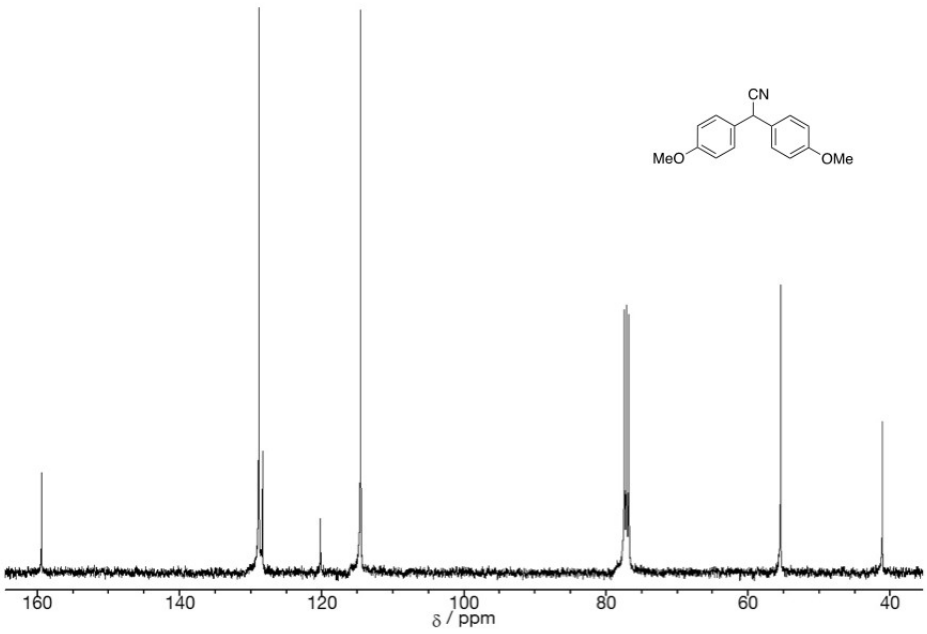

Figure S29. ^{13}C NMR spectrum of **DAAN-OMe** (125 MHz, $CDCl_3$).

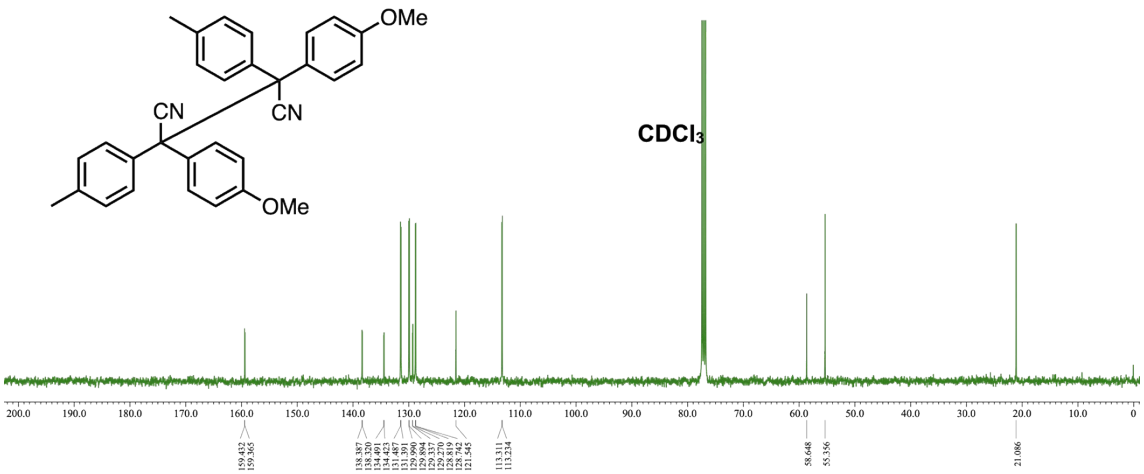

Figure S30. ^{13}C NMR spectrum of **TASN-Me** (125 MHz, $CDCl_3$).

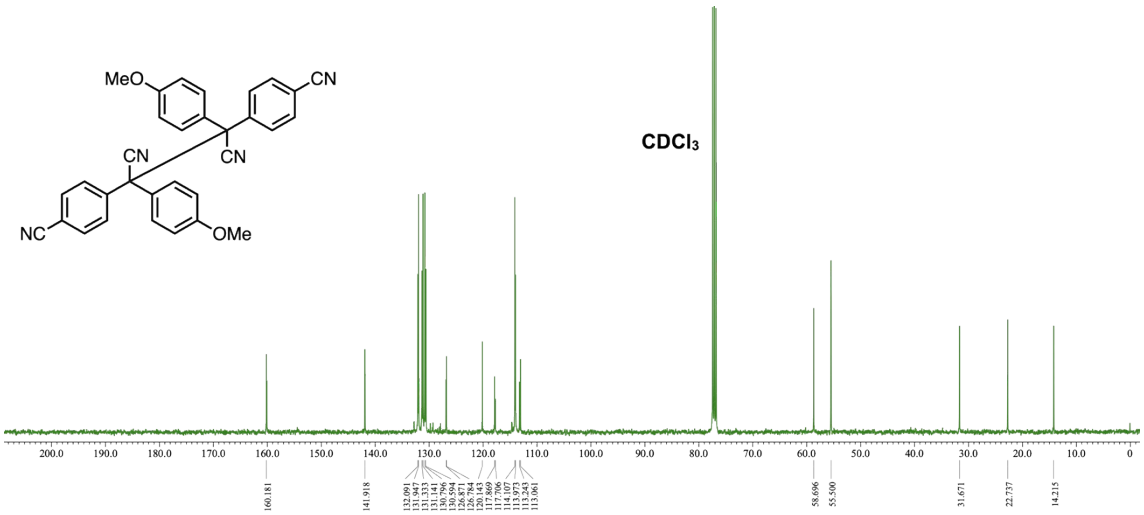

Figure S31. ^{13}C NMR spectrum of **TASN-CN** (125 MHz, $CDCl_3$).

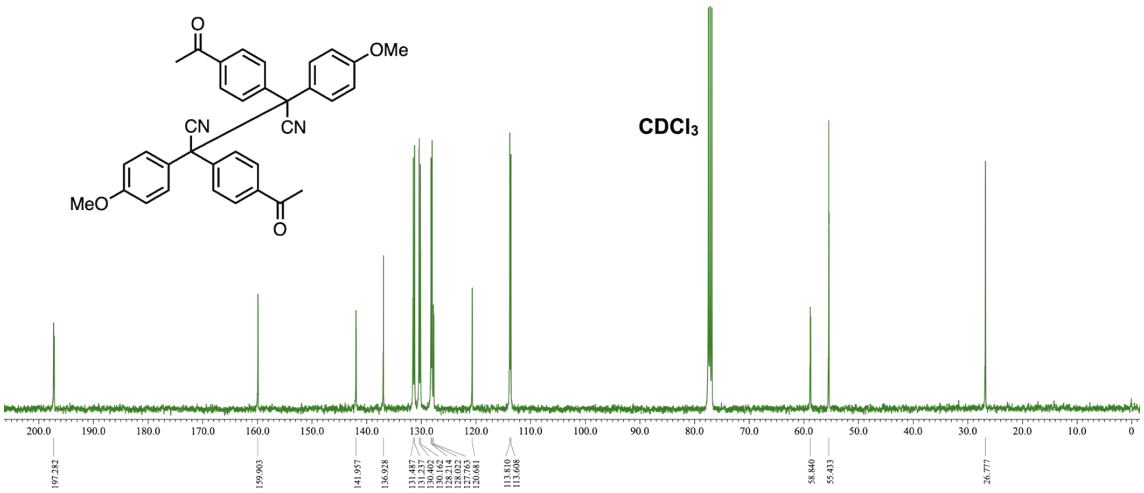

Figure S32. ^{13}C NMR spectrum of **TASN-Ac** (125 MHz, $CDCl_3$).

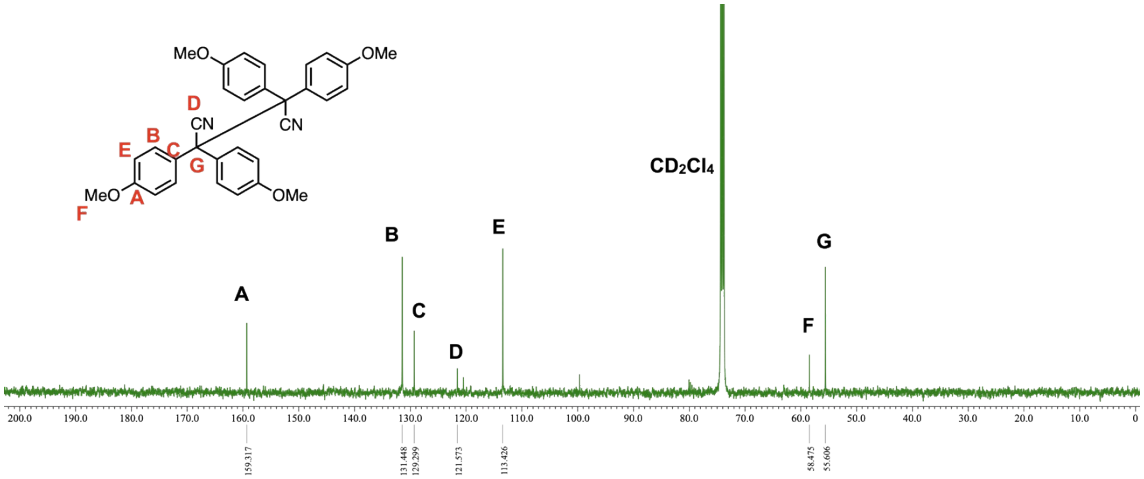

Figure S33. ^{13}C NMR spectrum of **TASN-OMe** (125 MHz, 1,1,2,2-tetrachloroethane-d_2).

4. GPC Curves

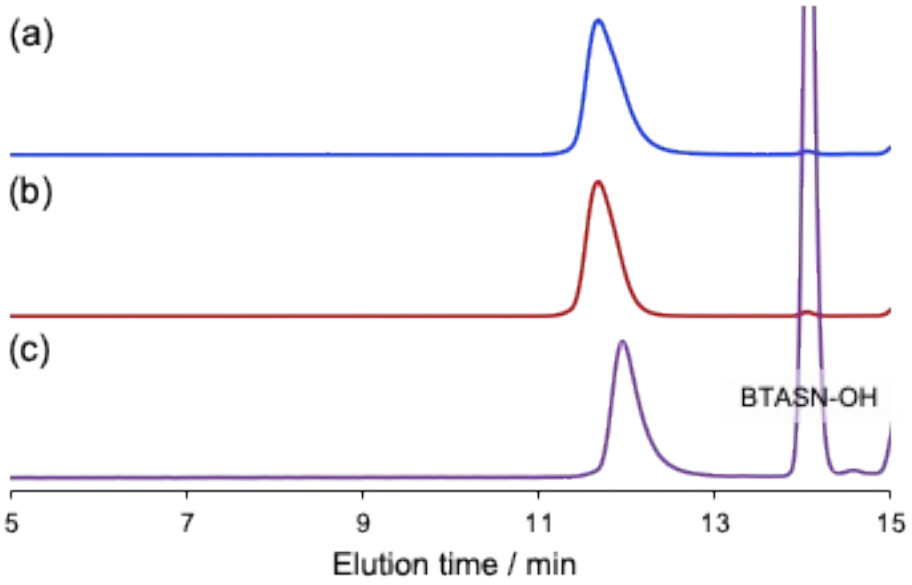

Figure S34. GPC curves (RI, THF) of (a) **BTASN-PMMA-Br** (M_n = 14,200, M_w/M_n = 1.14), (b) **BTASN-PMMA-H** (M_n = 16,000, M_w/M_n = 1.08), and (c) **BTASN-PMMA-H/OH** (40.9 mg, M_n = 9,790, M_w/M_n = 1.10).

5. EPR measurement

5. 1. Solution state EPR

50 mM **BTASN-OH** in anisole solution was transferred into an ESR glass capillary, and the capillary was sealed after being degassed via three times of freeze-pump-thaw cycling. The spectra were recorded using a microwave of 0.2 mW and a field modulation 0.1 mT with a time constant of 0.03 s. The sweep rate was 0.25 mT/s. In variable temperature measurements from 50 to 130 °C, the spectra were measured after waiting for 1 min at each temperature. The 2nd and 3rd cycles were started after cooling to 50 °C following the previous cycle, and waiting for 5 min. After performing measurements, following breaking capillary, the inside diameter was measured. The detection volume was calculated based on the measurement range and inside diameter. The amount of the radicals was determined by comparing the integration of the observed integral spectrum with a 0.01 mM solution of 4-hydroxy-2,2,6,6-tetramethylpiperidin-1-oxyl (TEMPOL) in anisole at 130 °C. The Mn^{2+} signal was used as an auxiliary standard. The g value was calculated according to the following equation:

$$g = h\nu/\beta H$$

where h is the Planck constant, ν is the microwave frequency, β is the Bohr magneton, and H is the magnetic field.

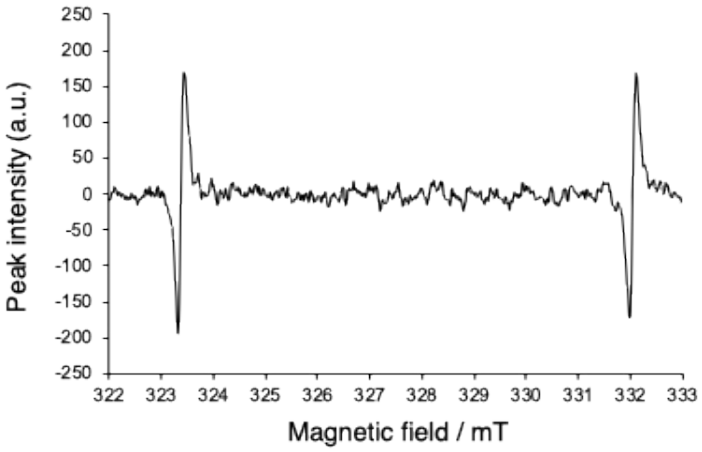

Figure S35. EPR spectrum of **BTASN-OH** in anisole 50 mM solution at 25 °C.

Thermal stability of TASN series

About 5 mM anisole solutions of s-dimers were charged in a 3 mm glass capillary with more than 43.5 mm height (effective measuring range), which was then sealed after freeze-thaw cycles. In all the cases, the *g*-values of radical signals were determined as 2.003, suggesting the signals observed were carbon-centered radicals. The dissociation constants K_d were calculated, of which the natural logarithms ln K_d, were plotted against $1/T$, where T is the absolute temperature in kelvin.

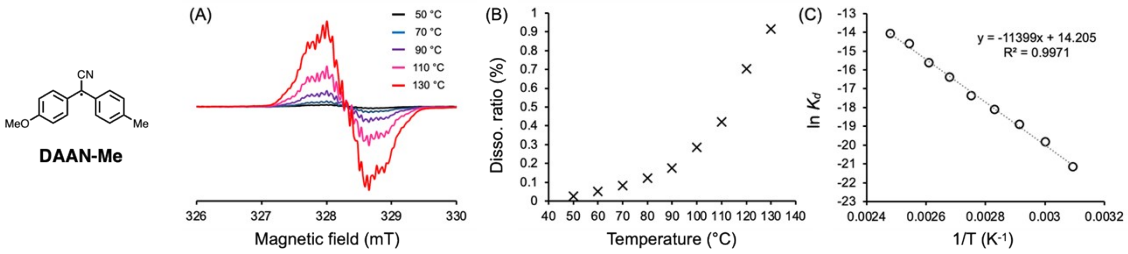

Figure S36. VT-EPR measurement of **TASN-Me**: (A) EPR profiles at elevated temperature, (B) dissociation ratios plotted with temperature, (C) van't Hoff plot.

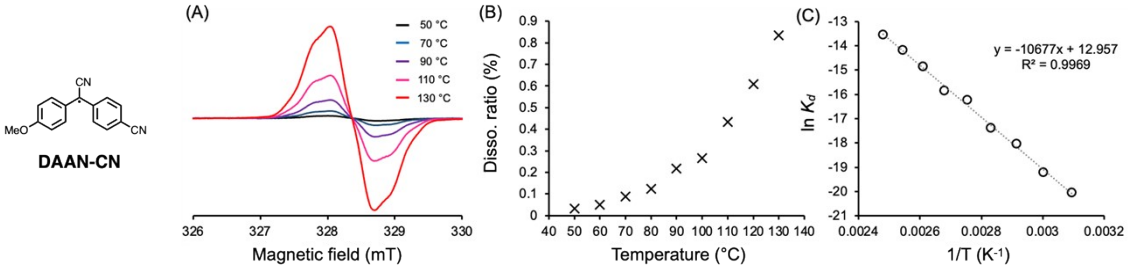

Figure S37. VT-EPR measurement of **TASN-CN**: (A) EPR profiles at elevated temperature, (B) dissociation ratios plotted with temperature, (C) van't Hoff plot.

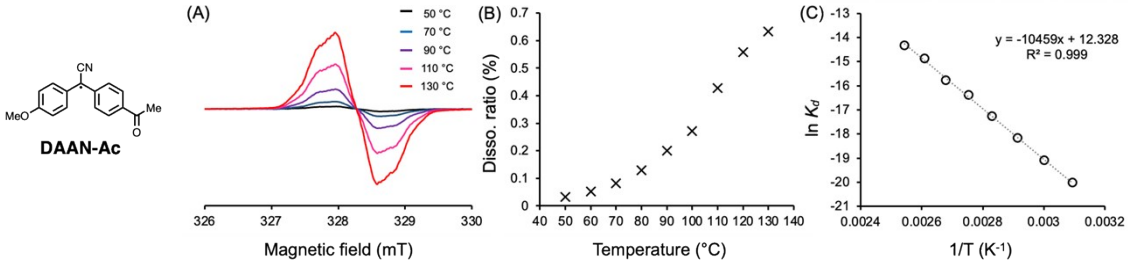

Figure S38. VT-EPR measurement of **TASN-Ac**: (A) EPR profiles at elevated temperature, (B) dissociation ratios plotted with temperature, (C) van't Hoff plot.

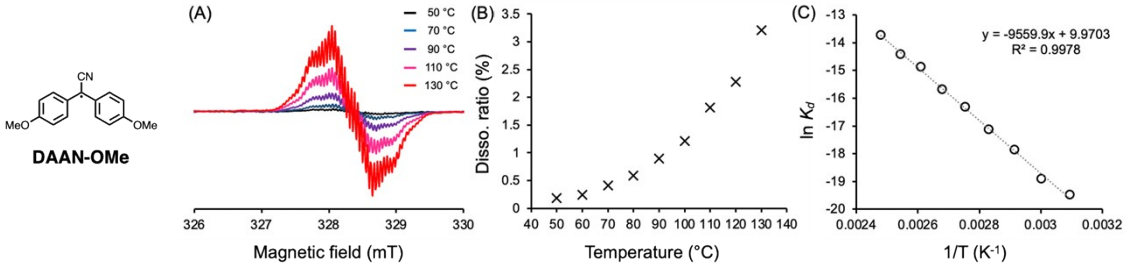

Figure S39. VT-EPR measurement of **TASN-OMe**: (A) EPR profiles at elevated temperature, (B) dissociation ratios plotted with temperature, (C) van't Hoff plot.

5. 2. Solid state EPR

The samples before or after grinding were transferred into an ESR glass capillary and weighed, and the capillary was sealed after being degassed. The spectra were recorded using a microwave of 0.2 mW and a field modulation 0.1 mT with a time constant of 0.03 s. The sweep rate was 0.25 mT/s. The amount of the radicals was determined by comparing the integration of the observed integral spectrum with a 0.01 mM solution of TEMPOL in benzene at room temperature. Likewise, the Mn^{2+} signal was used as an auxiliary standard, and the *g* value was calculated.

6. Computational detail

Optimization and CoGEF calculation

DFT calculations were performed using Q-Chem 6.1.1 program package. Geometry optimizations and vibrational analyses of all local equilibrium structures were performed using unrestricted B3LYP/6-31G(d,p). Structure of mechanophores were obtained by geometry optimization, potential energy surface search of C–C bonding rotation, and optimization of global minimum structure.

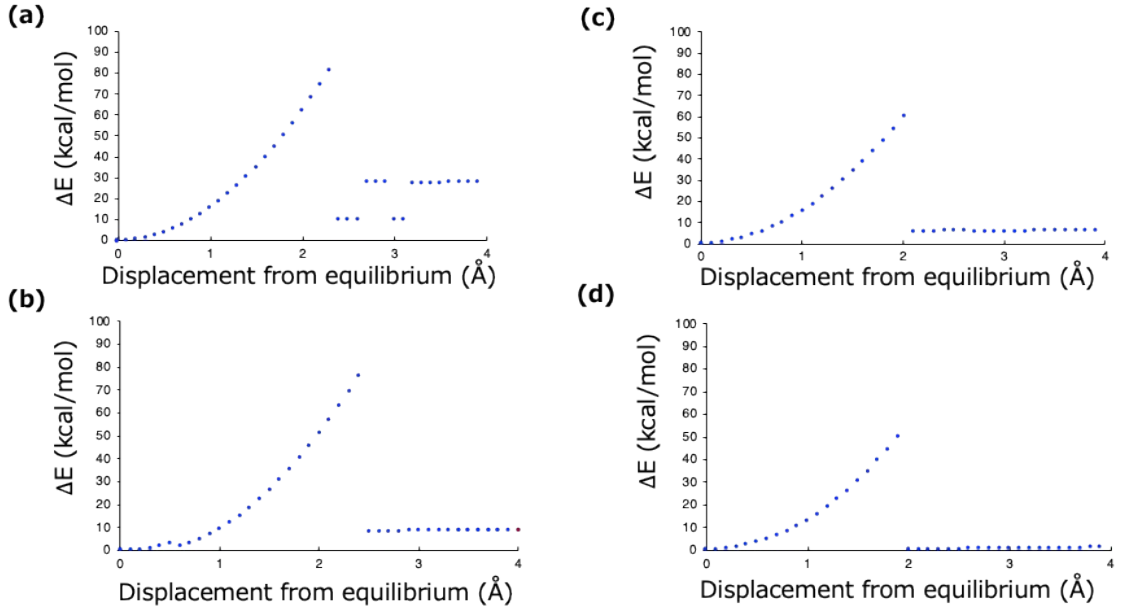

Figure S40. CoGEF calculation of (a) **BTASN-COOMe**, (b) **BTASN-CH_2OMe**, (c) **BTASN-OMe** and (d) **BTASN-NMe_2** under force (B3LYP/6-31G(d,p)).

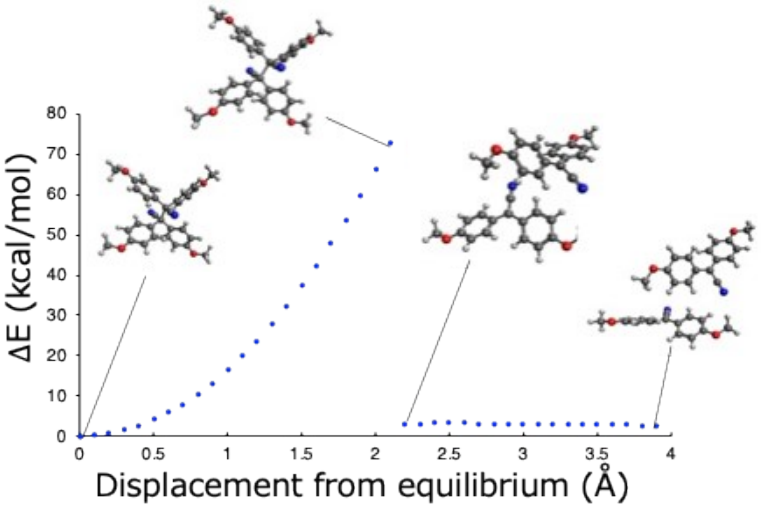

Figure S41. CoGEF calculation of **TASN** under force (B3LYP/6-31G(d,p)).

Molecular dynamics simulation using universal neural network potential

Before the simulation, Atactic PMMA 5mers and PS 5mers were generated from bifunctionalized ATRP initiators consisting of the mechanophores using SMARTS model implemented in rdkit. In all of the calculation, we used universal neural network potential implemented in Matlantis program package.[5] We carried out geometry optimization of the model polymers using LBFGASEOptFeature with EstimatorCalcMode.MOLECULE v6.0.0 as the PFP potential. After the calculation, NVT calculation was carried (Time step: 1.0, temperature: 300K, num_md_steps: 10,000 (10 ps), num_interval: 1000 (1 ps)) to obtain the corresponding equilibrium structures. After the equilibrium calculation, further NVT calculation (Time step: 1.0, temperature: 300K, num_md_steps: 1,500,000 (1.5 ns), num_interval: 1000 (1 ps)) was performed under force, in which pulling atoms were set at carbon atoms of the both polymer end groups and pulled at every 0.1 nN. EstimatorCalcMode. CRYSTAL_PLUS_D3 v6.0.0 was used for all of the NVT calculation. The resultant trajectories were visualized using Avogadro.[6]

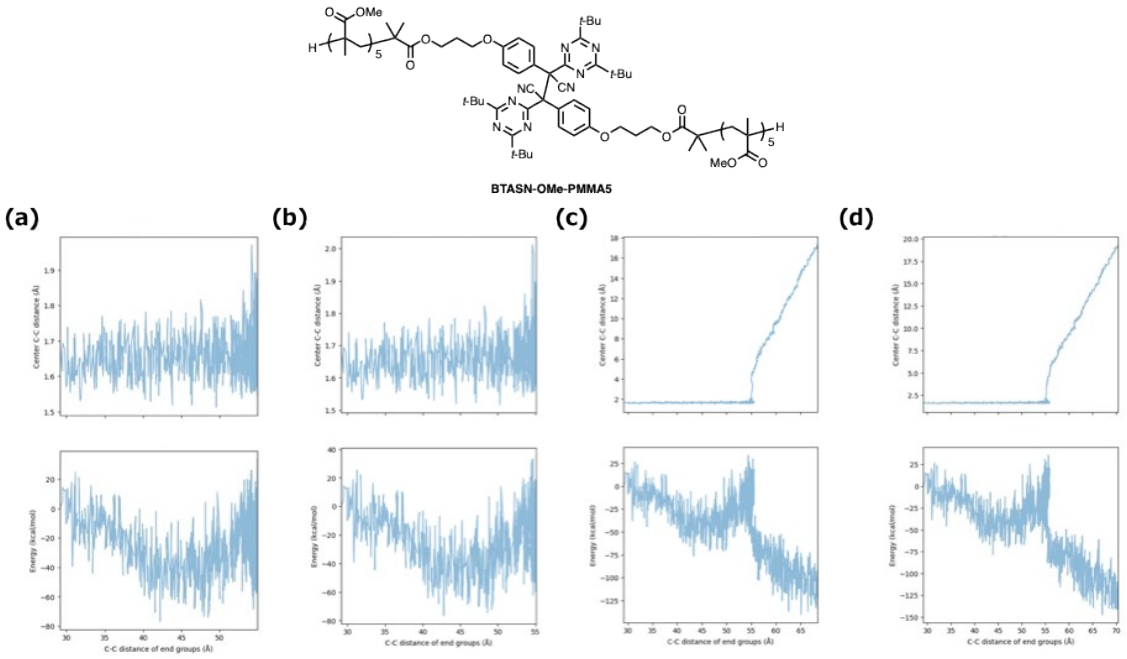

Figure S42. Summary of the MD calculation of **BTASN-OMe-PMMA5mers** using a universal neural network potential. The C-C distance of the end group *vs* the central C-C distance of the mechanophore and potential energy respectively at (a) 0.21 nN, (b) 0.22 nN, (c) 0.23 nN and (d) 0.24 nN.

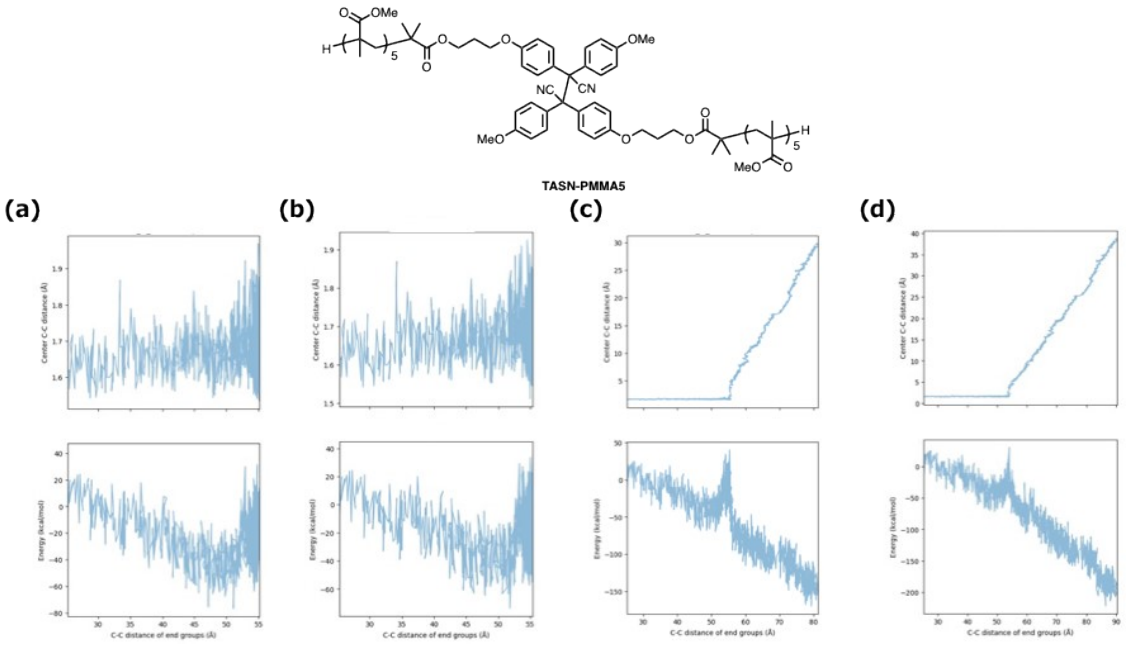

Figure S43. Summary of the MD calculation of **TASN -PMMA5mers** using an universal neural network potential. The C-C distance of the end group *vs* the central C-C distance of the

mechanophore and potential energy respectively at (a) 0.21 nN, (b) 0.22 nN, (c) 0.23 nN and (d) 0.24 nN.

TD-DFT calculation

TD-DFT calculations were performed using Gaussian16 program package.[2] Geometry optimizations and vibrational analyses of all local equilibrium structures were performed using unrestricted unrestricted B3LYP/6-31G(d,p). The geometries of the compounds were optimized without symmetry constraints. Calculations were performed using the unrestricted CAM-B3LYP with the 6-311+G(d,p) basis set. Frequency calculations were carried out to ensure that the optimized geometries were minima on the potential energy surface, in which no imaginary frequencies were observed in any of the compounds. TD-DFT calculations were performed using the unrestricted CAM-B3LYP with the 6-311+G(d,p) to calculate the first 5 doublet transitions. Cartesian coordinates and energies of the computed structures are listed as shown below.

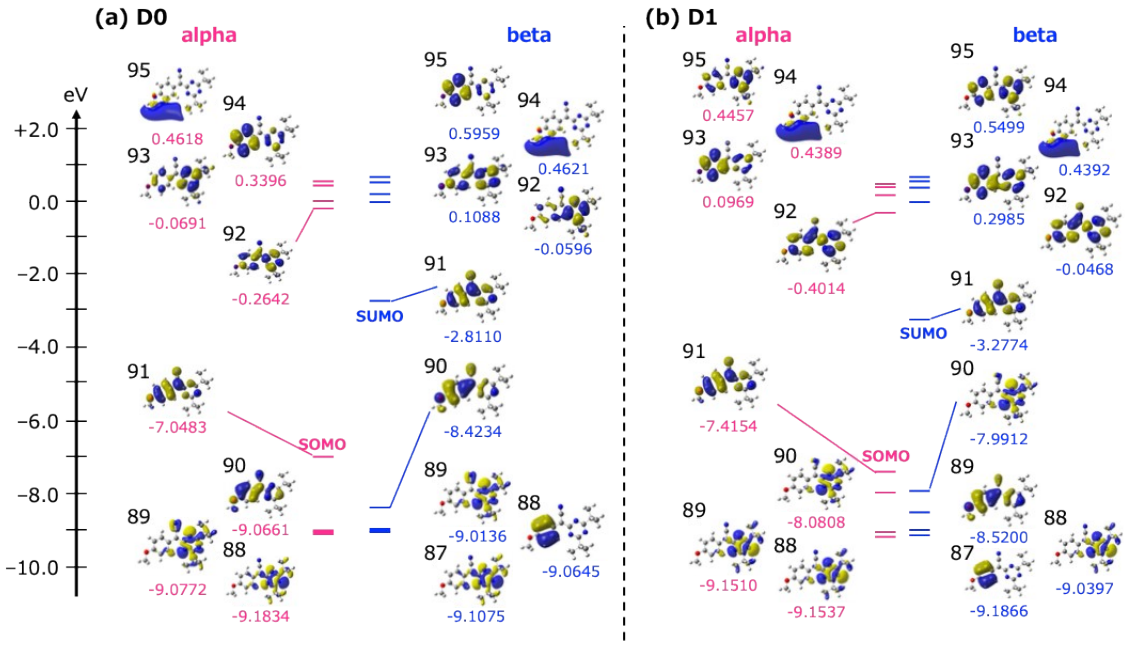

Figure S44. The results of TD-DFT simulation of **TAAN radical**. SUMO and SOMO stand for the lowest singly unoccupied molecular orbital and the highest singly occupied molecular orbital, respectively.

Table S1. Summary of TD-DFT calculation of **TAAN radical** ('up' = A, and 'down' = B)

Transition	Wavelength (nm)	Oscillator strength (*f*)	Orbital excitation contribution	Contribution (%)
D0 → D1	466.41	0.1664	91A → 92A	3.99
			91A → 97A	3.50
			82B → 91B	1.07
			90B → 91B	90.10
			90B → 93B	1.33
D1→ D0	970.04	0.0000	90B ← 91B	96.06
			90B ← 92B	3.94

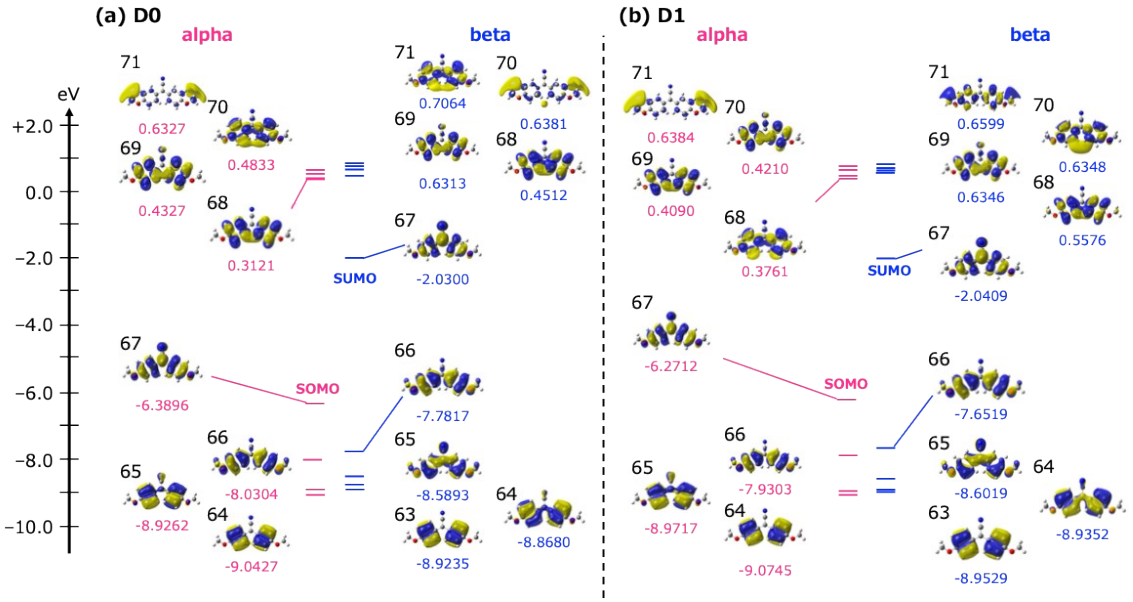

Figure S45. The results of TD-DFT simulation of **DAAN radical**. SUMO and SOMO stand for the lowest singly unoccupied molecular orbital and the highest singly occupied molecular orbital, respectively.

Table S2. Summary of TD-DFT calculation of **DAAN radical** (‘up’ = A, and ‘down’ = B)

Transition	Wavelength (nm)	Oscillator strength (*f*)	Orbital excitation contribution	Contribution (%)
D0 → D1	447.64	0.1091	66A → 74A	1.74
			67A → 70A	14.88
			60B → 67B	1.75
			65B → 71B	2.71
			66B → 67B	72.13
D1→ D0	473.93	0.1015	66A ← 74A	1.87
			67A ← 68A	15.96
			60B ← 67B	1.88
			65B ← 70B	2.90
			66B ← 67B	77.39

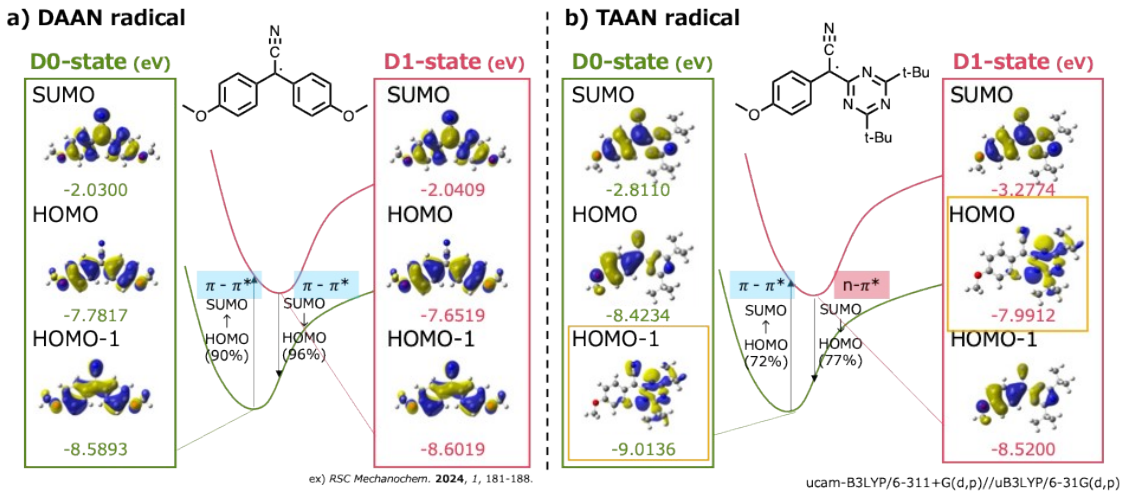

Figure S46. Schematic illustration of the results of TD-DFT simulation of results for a) **DAAN radical** and b) **TAAN radical**, with the key orbitals extracted. SUMO and SOMO stand for the lowest singly unoccupied molecular orbital and the highest singly occupied molecular orbital, respectively.

Cartesian coordinates and energies

TAAN-OMe radical D0

HF=-1071.4362734

Zero-point correction=0.417415

Thermal correction to Energy= 0.443127

Thermal correction to Enthalpy=0.444071

Thermal correction to Gibbs Free Energy=0.359821

Sum of electronic and zero-point Energies=-1071.018858

Sum of electronic and thermal Energies=-1070.993147

Sum of electronic and thermal Enthalpies=-1070.992202

Sum of electronic and thermal Free Energies=-1071.076452

C 0.4474750000 -0.6125120000 -0.0001460000
C -0.7646020000 -1.4321020000 -0.0000480000
C -2.1404480000 -0.9970050000 0.0000260000
C -0.5253910000 -2.8365610000 0.0000360000
N -0.4104030000 -3.9982930000 0.0000650000
C -2.5359240000 0.3667940000 -0.0001250000
C -3.8730780000 0.7358140000 -0.0000780000
C -4.8774530000 -0.2455940000 0.0001110000
C -4.5126890000 -1.6067910000 0.0003040000
C -3.1849960000 -1.9704070000 0.0002580000
N 0.3732140000 0.7332520000 -0.0001990000
C 1.5444500000 1.3797130000 -0.0000390000
N 2.7408360000 0.7754840000 0.0000430000
C 2.7244210000 -0.5698290000 -0.0001020000
N 1.6097500000 -1.2997850000 -0.0001200000
O -6.2072430000 0.0063650000 0.0001570000
C 1.5503170000 2.9102960000 0.0000950000
C 4.0766760000 -1.2821970000 -0.0000970000
H -1.7684940000 1.1270100000 -0.0002910000
H -4.1262140000 1.7892130000 -0.0001230000
H -5.2993320000 -2.3535220000 0.0004740000
H -2.9274430000 -3.0235020000 0.0004050000
C 3.9037650000 -2.8091350000 -0.0007340000
C 4.8555470000 -0.8425950000 1.2614510000

C 4.8561940000 -0.8416040000 -1.2608920000
C 0.1251900000 3.4840690000 -0.0001400000
C 2.3048170000 3.3915770000 -1.2609030000
C 2.3042850000 3.3912440000 1.2615330000
H 0.1717570000 4.5780540000 -0.0001080000
H -0.4350370000 3.1674030000 0.8841860000
H -0.4347370000 3.1674110000 -0.8846530000
H 2.3627300000 4.4847520000 1.2662220000
H 3.3189320000 2.9875330000 1.2858610000
H 1.7874250000 3.0773580000 2.1748550000
H 2.3632980000 4.4850810000 -1.2652450000
H 1.7883020000 3.0779610000 -2.1745110000
H 3.3194560000 2.9878330000 -1.2849290000
H 3.3525680000 -3.1519190000 0.8783850000
H 4.8890130000 -3.2871140000 -0.0006260000
H 3.3531000000 -3.1512480000 -0.8804520000
H 4.3349430000 -1.1515670000 2.1741950000
H 4.9806680000 0.2426210000 1.2869890000
H 5.8465710000 -1.3082520000 1.2660160000
H 4.3359930000 -1.1497290000 -2.1741490000
H 5.8471630000 -1.3073800000 -1.2653770000
H 4.9814600000 0.2436150000 -1.2854490000
C -6.6495590000 1.3602290000 -0.0004490000
H -6.3062190000 1.8924340000 -0.8951760000
H -6.3068660000 1.8930130000 0.8941870000
H -7.7388420000 1.3169930000 -0.0008310000

TAAN-OMe radical D1

HF=-1071.4072777
Zero-point correction=0.416761 (Hartree/Particle)
Thermal correction to Energy=0.442622
Thermal correction to Enthalpy=0.443566
Thermal correction to Gibbs Free Energy=0.358686
Sum of electronic and zero-point Energies=-1070.961813
Sum of electronic and thermal Energies=-1070.935953
Sum of electronic and thermal Enthalpies=-1070.935009

Sum of electronic and thermal Free Energies=-1071.019889

C 0.3800410000 -0.6727290000 0.0000400000
C -0.7474990000 -1.4656600000 0.0000330000
C -2.1489510000 -1.0195790000 0.0000170000
C -0.4835430000 -2.8656230000 0.0000180000
N -0.2702070000 -4.0126660000 0.0000640000
C -2.5436040000 0.3312230000 0.0003140000
C -3.8867710000 0.7048190000 0.0002920000
C -4.8882440000 -0.2725010000 -0.0000270000
C -4.5180990000 -1.6258400000 -0.0003150000
C -3.1826100000 -1.9867790000 -0.0002920000
N 0.4583810000 0.6967320000 0.0000420000
C 1.5757260000 1.3899590000 -0.0000120000
N 2.8106390000 0.8526760000 -0.0000230000
C 2.7755240000 -0.4998720000 0.0000070000
N 1.6635660000 -1.1779810000 0.0000330000
O -6.2284990000 -0.0191380000 -0.0000770000
C 1.4899680000 2.9251120000 -0.0000800000
C 4.1067920000 -1.2626740000 0.0000310000
H -1.7952300000 1.1109090000 0.0005810000
H -4.1368090000 1.7591570000 0.0005360000
H -5.2995290000 -2.3784330000 -0.0005580000
H -2.9229130000 -3.0402130000 -0.0005180000
C 3.8776760000 -2.7836520000 -0.0001730000
C 4.8873860000 -0.8409670000 1.2642190000
C 4.8876510000 -0.8406770000 -1.2638950000
C 0.0334430000 3.4157790000 0.0000640000
C 2.2160250000 3.4379390000 -1.2637920000
C 2.2163260000 3.4380930000 1.2633950000
H 0.0185710000 4.5100500000 -0.0000310000
H -0.5067580000 3.0710110000 0.8864690000
H -0.5069940000 3.0708490000 -0.8861330000
H 2.2055110000 4.5328900000 1.2715290000
H 3.2531070000 3.0965000000 1.2832360000
H 1.7198440000 3.0893280000 2.1748860000

H 2.2051960000 4.5327350000 -1.2720660000
H 1.7193360000 3.0890490000 -2.1751220000
H 3.2528080000 3.0963620000 -1.2838240000
H 3.3197080000 -3.1082620000 0.8823800000
H 4.8442320000 -3.2965540000 -0.0001250000
H 3.3199180000 -3.1080430000 -0.8829410000
H 4.3544140000 -1.1333780000 2.1746650000
H 5.0449190000 0.2394440000 1.2864400000
H 5.8622730000 -1.3390880000 1.2702880000
H 4.3548550000 -1.1328480000 -2.1745220000
H 5.8625230000 -1.3388280000 -1.2698930000
H 5.0452100000 0.2397340000 -1.2858280000
C -6.6566070000 1.3334740000 0.0001270000
H -6.3096780000 1.8680540000 -0.8933970000
H -6.3099200000 1.8677080000 0.8939540000
H -7.7470510000 1.3045790000 -0.0000240000

DAAN radical D0

HF=-823.2956802
Zero-point correction=0.261399
Thermal correction to Energy=0.278445
Thermal correction to Enthalpy=0.279389
Thermal correction to Gibbs Free Energy=0.214988
Sum of electronic and zero-point Energies=-823.034281
Sum of electronic and thermal Energies=-823.017235
Sum of electronic and thermal Enthalpies=-823.016291
Sum of electronic and thermal Free Energies=-823.080692

C 0.0000020000 1.1363200000 0.0000210000
C -1.2955970000 0.4724570000 -0.0403940000
C 1.2956010000 0.4724890000 0.0404930000
C -0.0000250000 2.5523990000 -0.0000860000
N -0.0000150000 3.7229120000 -0.0000960000
C 2.4609870000 1.1433960000 -0.3932820000
C 3.7146340000 0.5451910000 -0.3491530000

C 3.8472180000 -0.7597000000 0.1474280000
C 2.7068650000 -1.4394540000 0.6084430000
C 1.4628320000 -0.8373700000 0.5582390000
C -1.4628290000 -0.8373670000 -0.5582260000
C -2.7068620000 -1.4394430000 -0.6084680000
C -3.8472080000 -0.7597260000 -0.1473780000
C -3.7146180000 0.5451240000 0.3493130000
C -2.4609730000 1.1433350000 0.3934430000
O 5.0198200000 -1.4426350000 0.2357740000
C 6.2121900000 -0.7996130000 -0.1949830000
O -5.0197940000 -1.4426800000 -0.2357000000
C -6.2122190000 -0.7995400000 0.1947290000
H 4.5762680000 1.0979770000 -0.7034340000
H 2.8304370000 -2.4359490000 1.0192920000
H 0.6073330000 -1.3672570000 0.9604370000
H -0.6073250000 -1.3672130000 -0.9604760000
H -2.8304390000 -2.4358960000 -1.0194130000
H -4.5762620000 1.0978850000 0.7036140000
H -2.3745770000 2.1533920000 0.7811290000
H 7.0156800000 -1.5187180000 -0.0320370000
H 6.1684370000 -0.5412600000 -1.2601600000
H 6.4140030000 0.1071950000 0.3882040000
H -6.4137110000 0.1073530000 -0.3884260000
H -6.1687870000 -0.5413040000 1.2599530000
H -7.0157480000 -1.5185270000 0.0314590000
H 2.3746080000 2.1534750000 -0.7809130000

DAAN radical D1

HF=-823.2934928
Zero-point correction=0.258808
Thermal correction to Energy=0.276288
Thermal correction to Enthalpy=0.277232
Thermal correction to Gibbs Free Energy=0.211934
Sum of electronic and zero-point Energies=-822.945487
Sum of electronic and thermal Energies=-822.928006

Sum of electronic and thermal Enthalpies=-822.927062
Sum of electronic and thermal Free Energies=-822.992361

C -0.0000020000 1.1039770000 -0.0000860000
C -1.2889800000 0.4495010000 -0.0298280000
C 1.2889630000 0.4494620000 0.0296530000
C 0.0000180000 2.5187060000 -0.0000420000
N 0.0000700000 3.6904930000 0.0000470000
C 2.4785040000 1.1620790000 -0.3523480000
C 3.7317910000 0.5890470000 -0.3005610000
C 3.8800980000 -0.7460670000 0.1375970000
C 2.7291620000 -1.4698300000 0.5434100000
C 1.4815680000 -0.8923900000 0.4962670000
C -1.4816370000 -0.8922910000 -0.4966040000
C -2.7292270000 -1.4697670000 -0.5435780000
C -3.8800930000 -0.7460840000 -0.1374740000
C -3.7317540000 0.5890190000 0.3007360000
C -2.4784770000 1.1620800000 0.3523550000
O 5.0551720000 -1.4221650000 0.2097540000
C 6.2525610000 -0.7599400000 -0.1821340000
O -5.0551560000 -1.4222400000 -0.2093490000
C -6.2525710000 -0.7598550000 0.1821630000
H 4.5930710000 1.1716050000 -0.6065390000
H 2.8637230000 -2.4843690000 0.9047290000
H 0.6319660000 -1.4562020000 0.8609610000
H -0.6320910000 -1.4560040000 -0.8615820000
H -2.8638190000 -2.4842550000 -0.9050290000
H -4.5930040000 1.1715370000 0.6068710000
H -2.3776130000 2.1874930000 0.6907350000
H 7.0546770000 -1.4849960000 -0.0427320000
H 6.2134050000 -0.4563340000 -1.2349040000
H 6.4434700000 0.1204370000 0.4427310000
H -6.4432180000 0.1204910000 -0.4428250000
H -6.2136780000 -0.4561620000 1.2349200000
H -7.0547300000 -1.4848390000 0.0426320000
H 2.3776690000 2.1875040000 -0.6906970000

7. Correlation between computational values of RSE and experimental values of ln K_d

The natural logarithms of K_d (ln K_d) at 100 °C in anisole of each compound were listed together with the computational results of RSE in **Table S3**. RSE values were calculated based on an isodesmic hydrogen-atom transfer reaction using the methyl radical as a reference, according to the following equation:

$$RSE = E(R^{\cdot}) + E(CH4) - E(RH) - E(CH3^{\cdot})$$

Table S3. Computational results of RSE; experimental facts of ln Kd (100 °C, anisole)

Carbon-centered radicals	RSE[a] (kJ / mol)	ln K_d @100 °C
BTASN-OMe	–140.25	–23.50
TASN-Me	–145.54	−16.33 ± 0.04
TASN-CN	–147.53	−15.79 ± 0.03
TASN-Ac	–148.12	−15.75 ± 0.05
TASN-OMe	–148.38	−15.69 ± 0.04
BiACA-NMe_2[b]	–145.34	–16.68 ± 0.05
BiACA-OMe[b]	–133.63	–21.58 ± 0.03
BiACA-Me[b]	–126.69	–26.20 ± 0.07
BiACA-H[b]	–122.85	–27.16 ± 0.09
BiACA-Ac[b]	–122.17	–28.42 ± 0.14
DATCE-COOMe	–153.50	–19.41[c]
DATCE-CN	–152.86	–19.01[c]
DATCE-Me	–157.08	–17.28[c]
DATCE-OMe	–163.24	–15.18[c]
DATCE-NMe_2	–175.07	–13.37[c]

[a] DFT calculation were performed at the unrestricted B3LYP/6-31++G(d,p) level.

[b] RSE and ln Kd values were taken from the literature.[7]

[c] The dissociation constants K_d were obtained as the reciprocal of the reported binding constants K_a,[8] which were measured in methanol or toluene at 50 °C and therefore differ from our experimental conditions.

References

[1] L. Hintermann, L. Xiao, A. Labonne, *Angew. Chem. Int. Ed,* **2008**, *47*, 8246.

[2] Gaussian 16, Revision C.01, M. J. Frisch, G. W. Trucks, H. B. Schlegel, G. E. Scuseria, M. A. Robb, J. R. Cheeseman, G. Scalmani, V. Barone, G. A. Petersson, H. Nakatsuji, X. Li, M. Caricato, A. V. Marenich, J. Bloino, B. G. Janesko, R. Gomperts, B. Mennucci, H. P. Hratchian, J. V. Ortiz, A. F. Izmaylov, J. L. Sonnenberg, D. Williams-Young, F. Ding, F. Lipparini, F. Egidi, J. Goings, B. Peng, A. Petrone, T. Henderson, D. Ranasinghe, V. G. Zakrzewski, J. Gao, N. Rega, G. Zheng, W. Liang, M. Hada, M. Ehara, K. Toyota, R. Fukuda, J. Hasegawa, M. Ishida, T. Nakajima, Y. Honda, O. Kitao, H. Nakai, T. Vreven, K. Throssell, J. A. Montgomery, Jr., J. E. Peralta, F. Ogliaro, M. J. Bearpark, J. J. Heyd, E. N. Brothers, K. N. Kudin, V. N. Staroverov, T. A. Keith, R. Kobayashi, J. Normand, K. Raghavachari, A. P. Rendell, J. C. Burant, S. S. Iyengar, J. Tomasi, M. Cossi, J. M. Millam, M. Klene, C. Adamo, R. Cammi, J. W. Ochterski, R. L. Martin, K. Morokuma, O. Farkas, J. B. Foresman and D. J. Fox, Gaussian, Inc., Wallingford CT, 2016.

[3] Y. Shao, Z. Gan, E. Epifanovsky, A. T. B. Gilbert, M. Wormit, J. Kussmann, A. W. Lange, A. Behn, J. Deng, X. Feng, D. Ghosh, M. Goldey, P. R. Horn, L. D. Jacobson, I. Kaliman, R. Z. Khaliullin, T. Kuś, A. Landau, J. Liu, E. I. Proynov, Y. M. Rhee, R. M. Richard, M. A. Rohrdanz, R. P. Steele, E. J. Sundstrom, H. L. Woodcock III, P. M. Zimmerman, D. Zuev, B. Albrecht, E. Alguire, B. Austin, G. J. O. Beran, Y. A. Bernard, E. Berquist, K. Brandhorst, K. B. Bravaya, S. T. Brown, D. Casanova, C.-M. Chang, Y. Chen, S. H. Chien, K. D. Closser, D. L. Crittenden, M. Diedenhofen, R. A. DiStasio Jr., H. Do, A. D. Dutoi, R. G. Edgar, S. Fatehi, L. Fusti-Molnar, A. Ghysels, A. Golubeva-Zadorozhnaya, J. Gomes, M. W. D. Hanson-Heine, P. H. P. Harbach, A. W. Hauser, E. G. Hohenstein, Z. C. Holden, T.-C. Jagau, H. Ji, B. Kaduk, K. Khistyaev, J. Kim, J. Kim, R. A. King, P. Klunzinger, D. Kosenkov, T. Kowalczyk, C. M. Krauter, K. U. Lao, A. D. Laurent, K. V. Lawler, S. V. Levchenko, C. Y. Lin, F. Liu, E. Livshits, R. C. Lochan, A. Luenser, P. Manohar, S. F. Manzer, S.-P. Mao, N. Mardirossian, A. V. Marenich, S. A. Maurer, N. J. Mayhall, E. Neuscamman, C. M. Oana, R. Olivares-Amaya, D. P. O'Neill, J. A. Parkhill, T. M. Perrine, R. Peverati, A. Prociuk, D. R. Rehn, E. Rosta, N. J. Russ, S. M. Sharada, S. Sharma, D. W. Small, A. Sodt, T. Stein, D. Stück, Y.-C. Su, A. J. W. Thom, T. Tsuchimochi, V. Vanovschi, L. Vogt, O. Vydrov, T. Wang, M. A. Watson, J. Wenzel, A. White, C. F. Williams, J. Yang, S. Yeganeh, S. R. Yost, Z.-Q. You, I. Y. Zhang, X. Zhang, Y. Zhao, B. R. Brooks, G. K.-L. Chan, D. M. Chipman, C. J. Cramer, W. A. Goddard III, M. S. Gordon, W. J. Hehre, A. Klamt, H. F. Schaefer III, M. W. Schmidt, C. D. Sherrill, D. G. Truhlar, A. Warshel, X. Xu, A. Aspuru-Guzik, R. Baer, A. T. Bell, N. A. Besley, J.-D. Chai, A. Dreuw, B. D. Dunietz, T. R. Furlani, S. R. Gwaltney, C.-P. Hsu, Y. Jung, J. Kong, D. S. Lambrecht, W. Liang, C. Ochsenfeld, V. A. Rassolov, L. V. Slipchenko, J. E. Subotnik, T. Van Voorhis, J. M. Herbert, A. I. Krylov, P. M. W. Gill and M. Head-Gordon, *Mol. Phys.* **2015**, *113*, 184.

[4] (a) C.-F. Huang, Y. Ohta, A. Yokoyama, T. Yokozawa, *Macromolecules* **2011**, *44*, 4140. (b)

X. Jiang, J. Han, L. Cao, Y. Bao, J. Shi, J. Zhang, L. Ni and J. Chen, *Polymers* **2017**, *10*, 26.

[5] S. Takamoto, C. Shinagawa, D. Motoki, K. Nakago, W. Li, I. Kurata, T. Watanabe, Y. Yayama, H. Iriguchi, Y. Asano, T. Onodera, T. Ishii, T. Kudo, H. Ono, R. Sawada, R. Ishitani, M. Ong, T. Yamaguchi, T. Kataoka, A. Hayashi, N. Charoenphakdee and T. Ibuka, *Nat. Commun.* **2022**, *13*, 2991.

[6] M. D. Hanwell, D. E. Curtis, D. C. Lonie, T. Vandermeersch, E. Zurek and G. R. Hutchison, *J. Cheminform.* **2012**, *4*, 17.